2015

A Hydrographic Climatology of the Gulf of St. Lawrence

Alejandro Frank
University of South Carolina - Columbia

A Hydrographic Climatology of the Gulf of St. Lawrence

by

Alejandro J. Frank

Bachelor of Science
University of South Carolina, 2001

Bachelor of Science
University of South Carolina, 2012

Submitted in Partial Fulfillment of the Requirements

For the Degree of Master of Science in

Marine Science

College of Arts and Sciences

University of South Carolina

2015

Accepted by:

Alexander Yankovsky, Director of Thesis

Howie Scher, Reader

Venkat Lakshmi, Reader

Lacy Ford, Vice Provost and Dean of Graduate Studies

DEDICATION

To my parents and family

ACKNOWLEDGEMENTS

I would like to thank my committee,

Dr. Igor Yashayaev and

Legna Torres

ABSTRACT

The Gulf of St. Lawrence (GSL) is characterized by a general circulation of an estuarine type, where fresher/lighter water flows seaward above saltier/heavier water flowing landward. In an estuarine regime, the inflowing deep layer water compensate for a loss of mass due to the surface layer outflow. A major element of the GSL estuarine circulation is the coastal buoyancy-driven current fed by the St. Lawrence River discharge. In addition, some surface water is advected into the GSL as a branch of the Labrador Current (LC). Recent climatological changes in the North Atlantic have increased the melting rate of the Greenland ice sheets, resulting in a freshening of the LC. NOAAs' National Oceanographic Data Center (NODC) hydrographic data, comprising salinity and temperature measurements in the GSL from 1950-2010 warm seasons, were used to construct three climatological transects across major branches of the estuarine circulation in the GSL. Each transect was then subdivided into three vertical layers representing distinct water masses in the GSL: a fresh and warm surface layer, a cold intermediate layer (CIL), and a warmer, salty Atlantic water bottom layer. The surface layer was further subdivided into boxes inside and outside of the coastal buoyancy-driven current. A climatology was constructed on a bi-monthly basis in order to assess and remove effects of the seasonal cycle on the annual anomaly estimates. Linear trends for temporal evolution of annual temperature and salinity anomalies were estimated. We

found a basin wide warming and salting of the bottom layer. Minimal change was found for the CIL. The surface layer showed a cooling and salting trend within the buoyancy-driven coastal current, while a warming and freshening trend was found in the rest of the surface layer; a signal of changes in the LC. Salinity trends in the buoyancy costal current cannot be deducted from annual variations of the St. Lawrence River discharge and could be explained by increased mixing. Entrainment of ambient water into a buoyancy current implies enhanced seaward transport, which leads to stronger near-bottom landward advection of Atlantic water into the GSL. The observed increase of stratification has strong implications for the GSL ecology. Our analysis suggests that global change trends can be amplified in semi-enclosed basins due to advective processes.

TABLE OF CONTENTS

LIST OF TABLES

LIST OF FIGURES

CHAPTER 1 INTRODUCTION AND BACKGROUND

1.1 INTRODUCTION AND MOTIVATION

The Gulf of St. Lawrence (GSL) is a semi enclosed basin. It receives and exchanges water through 3 water pathways, the first of which is through the St. Lawrence estuarine system, which is fed by the freshwater outflow of the Great Lakes from the St. Lawrence River. The second pathway is through the Strait of Belle Isle, where the entering water carries a strong signature from the Labrador Current (LC). The Labrador Current has been experiencing a freshening trend due to an increased melting rate of the Greenland Ice sheet. The third pathway is at the Cabot Strait (CS). Water on the shelf enters the GSL on the eastern side of the Laurentian Channel and shows a signature from the LC. In addition continental slope water (Atlantic water) is advected into the GSL at depth as a compensating flow. The vertical circulation pattern resembles a classic estuarine mixing regime, with freshwater overlaying an encroaching salt water wedge. Our goal was to establish the mean conditions for salinity and temperature over a specific time frame (referred to as a climatology) for vertical transects; to determine and possibly explain temporal trends over the same time interval. We approached the GSL as a perceived estuarine system. The selected transects were located in the GSL such as to encompass the above mentioned pathways. The chosen time frame was from 1950-2010. We found a well-defined buoyancy driven current associated with local buoyancy forcing (St. Lawrence River). This buoyancy driven current depicts a salting trend. We believe this

salting trend to be the result of increased atmospheric induced mixing rather than a result of changing freshwater discharge. We also found a freshening and warming trend in the rest of the GSL (excluding the buoyancy driven current), a signal stemming from the freshening of the LC (non-local forcing). The salting of the buoyancy driven current increases the volume of water that is advected at depth from the shelf break and upper continental slope. This is a result of the estuarine type circulation which is governed by conservation of mass and freshwater flux. Our analysis shows that global change trends can be enhanced in semi-enclosed basins due to advective processes.

The paper is organized as follows: Chapter one gives background information about the GSL, estuarine type circulation and transect placement. Chapter two describes the data analysis and chapter three gives the results and conclusion.

1.2 BASIN TOPOGRAPHY

The Gulf of St. Lawrence (GSL) is a semi enclosed shallow sea which encompasses approximately 235,000 km^2 and contains 35,000 km^3 of water (including St. Lawrence Estuary) (Galbraith et al. 2012) with a mean depth of 152 m (Ketchum 1983). It is flanked by Newfoundland in the east, Quebec on the north and the Nova Scotia peninsula on the southeast.

The GSL is a classic example of a drowned river valley. It was formed during the last ice age when sea level was about 100 m lower (Ketchum 1983) exposing parts of the now submerged continental shelf. Figure 1.2 shows the shoreline (thick line) in the GSL 13.000 – 10.000 years ago. Rivers and continental runoff cut canyons into the bedrock, and glaciers carved the Great Lakes, forming dams which periodically broke and discharged very large debris laden pulses of water. These events created torrential

outflows which eroded the canyons and riverbeds, forming the Laurentian channel (Shaw et al. 2002). Downriver of where the Saguenay River meets the St. Lawrence River (Fig. 1.1) the bathymetry deepens over a short distance of 20 km from a depth of 40 m to 350 m, called the Laurentian Trough. It becomes the Laurentian Channel further downstream (Ketchum 1983). At the Cabot Strait (CS) the Laurentian Channel deepens to 480 m (Galbraith et al. 2012) (Fig 1.3). The Laurentian channel, now the most prominent bathymetric feature, runs from the current St. Lawrence estuary in the northwestern corner through the center of the GSL basin, continues through the Cabot Strait and across the continental shelf to the continental slope, its total length is approximately 1400 km.

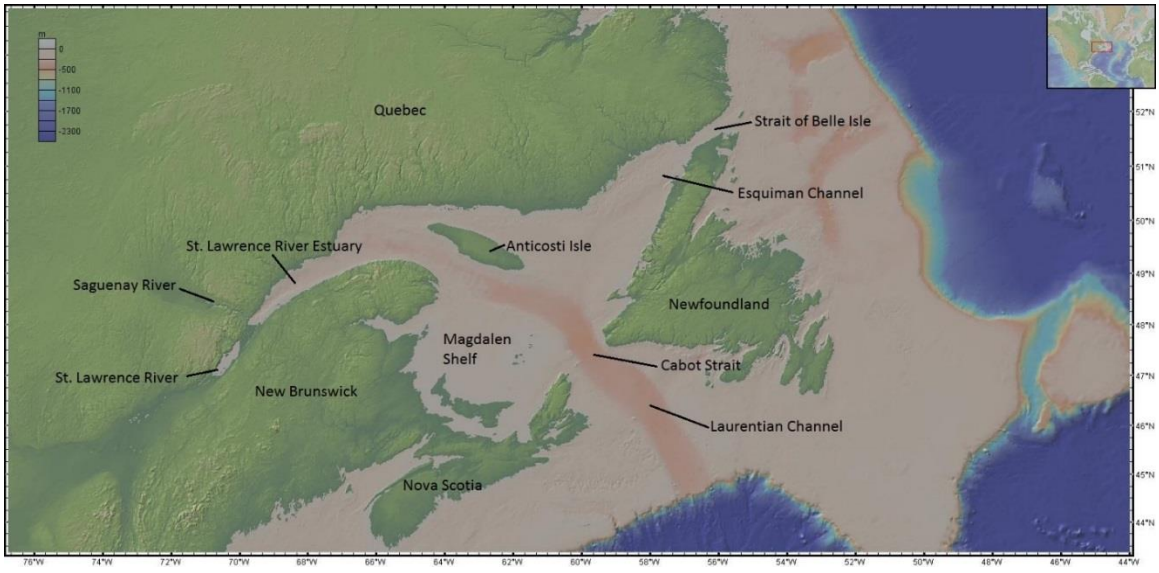

Figure 1.1: Location of the GSL with adjacent shelf adapted from GeoMapApp http://www.geomapapp.org

The Laurentian channel influences circulation patterns in the GSL, as does the Esquiman Channel running from the Strait of Belle Isle (SBI), which connects the GSL to the

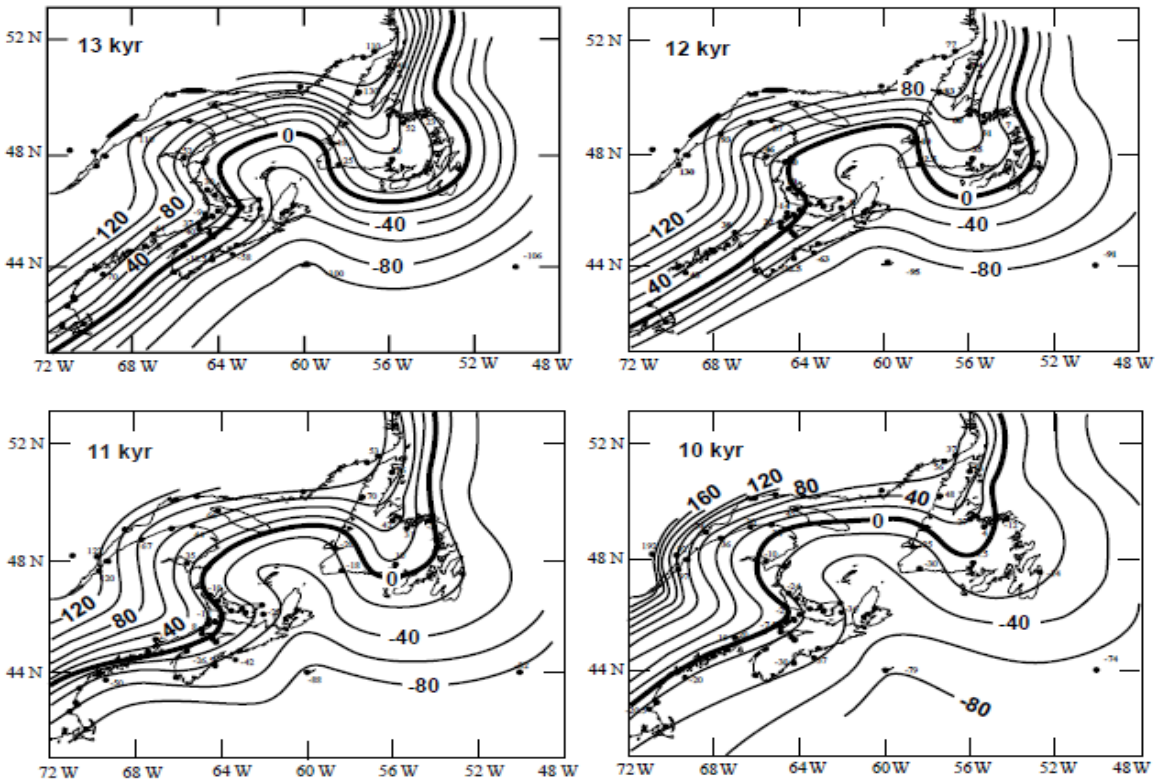

Figure 1.2: Bathymetry map 13 – 10 kyr, showing changes to shoreline location. Thick line depicting location of shoreline during last ice age. Negative contour lines indicate depth below sea surface, positive contour lines indicate elevation above sea surface from Shaw et al. 2002

Labrador Sea in the northeastern corner and runs southeast until it merges with the Laurentian Channel. The Magdalen Shallows are a shallow area (averaging < 80m) on the western side of the GSL, southward of the mouth of the St. Lawrence estuary and north of Nova Scotia (Fig. 1.1). The exiting waters of the St. Lawrence River separate into two

branches between the Anticosti Island and CS, one flowing over the Magdalen Shallows one continuing straight. These branches merge before crossing CS.

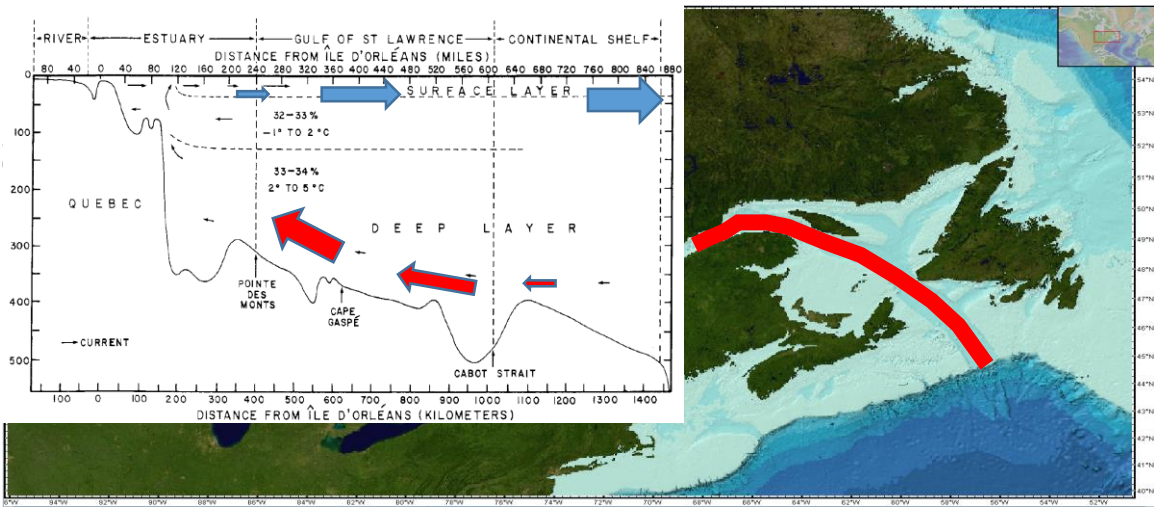

Figure 1.3: Longitudinal profile along the St. Lawrence channel (transect shown in map in red) to the edge of the continental shelf (adapted from GeoMappApp), also showing estuarine like circulation pattern, and 3 vertical layers, mixed surface layer, CIL, deep layer (Ketchum 1984). Arrows indicate surface flow (blue) and deep layer flow (red).

1.3 WATER MASSES

Most of the freshwater enters the GSL through the St. Lawrence Estuary which is the Great Lakes outflow (comprising 84% of the freshwater in the GSL according to Koutitonsky and Bugden 1991). El Sabh (1977) estimates the annual river discharge as 1.9×10^4 m^2 s^{-1}, while Saucier and Chassé (2000) estimated that discharge values to range from 1.1×10^4 m^3 s^{-1} up to 1.7×10^4 m^3 s^{-1} during spring freshet. In addition, 1.3×10^3 m^3 s^{-1} enter the GSL through the Saguenay River (Saucier and Chassé 2000), which when combined with other smaller contributories along the northern boundary equal 14% of the contributed freshwater (Koutitonsky and Bugden 1991). Figure 1.4, from Loder et

al. (1998), shows their estimated freshwater transport of the Labrador Current and estimated freshwater runoff into the GSL. All values are in millisverdrups.

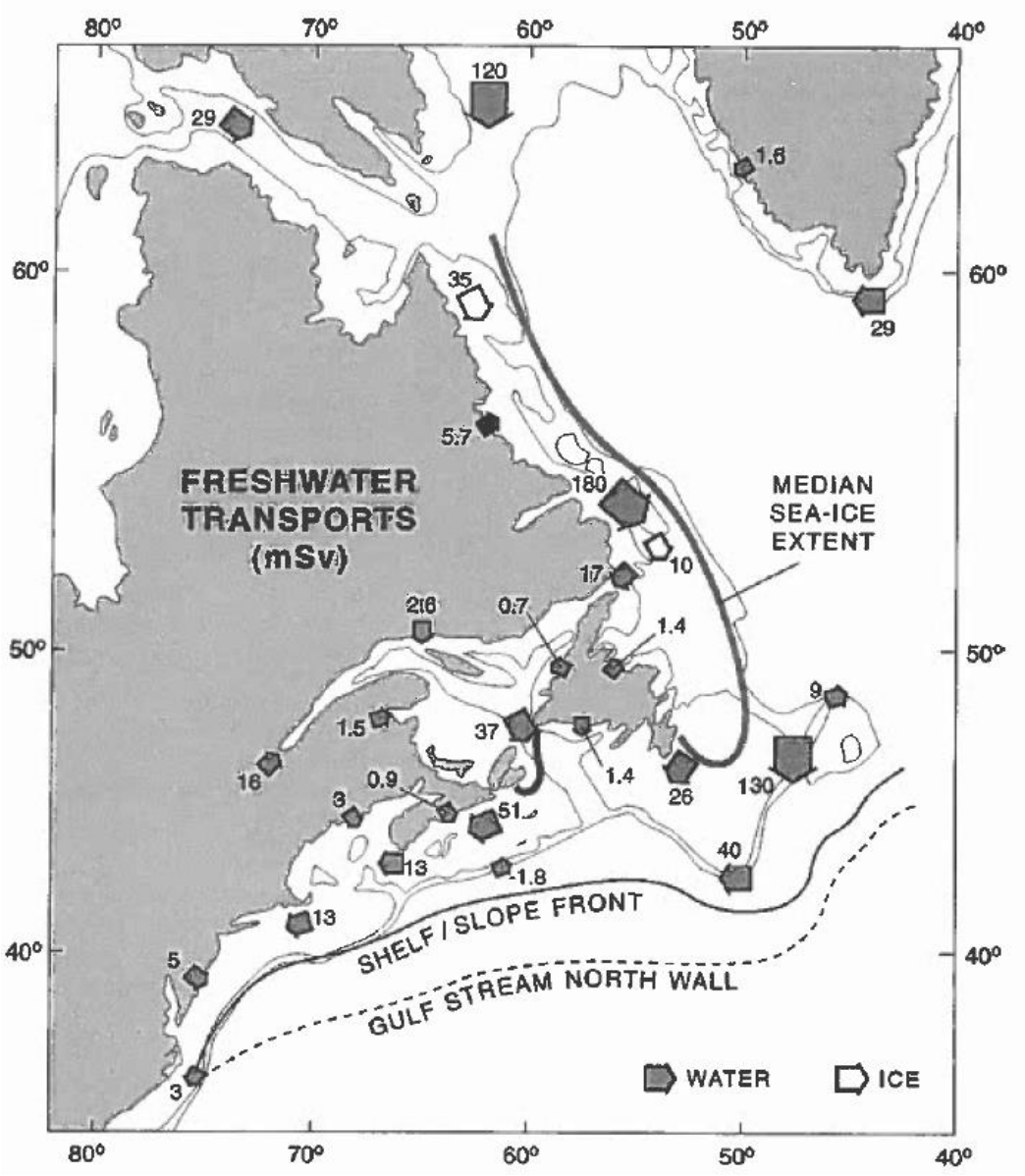

Figure 1.4: Freshwater transport in millisverdrups (mSv). Filled arrows depict ocean currents and continental runoff. Open arrows depict sea ice drift. From Loder et al. 1998

The GSL is connected to the Atlantic Ocean via the Cabot Strait, allowing approximately 0.5 Sv of oceanic water (Sv = Sverdrup 10^6 m^3 s^{-1}) to enter at depth and penetrate the channel (Khatiwala et al. 1999, Loder et al. 1998). In addition to the seawater entering from the Atlantic Ocean through the Laurentian Channel, a smaller but a still substantial amount of relatively fresh seawater from the LC enters through the SBI. The net flow has been estimated to range between 0.13 Sv (Galbraith 2006) (salinity ~ 31 psu) to 0.22 Sv (Khatiwala et al. 1999). Even though the SBI is much narrower (15-18 km) and shallower (<60 m) (Galbraith 2006) than CS, it is an important contributor to the circulation in the GSL (Fig. 1.5). While the exact role of these SBI water in the formation process of the cold intermediate layer (CIL) is not completely understood, most literature

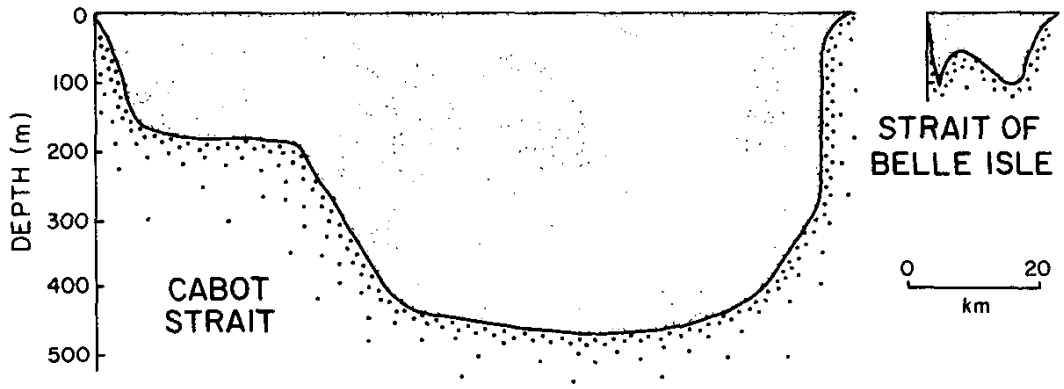

Figure 1.5: Cabot Strait and Strait of Belle Isle cross section from Garret et al 1980

agrees that the SBIs contribution is substantial. The cold waters entering from the Labrador Sea travel along the northern shoreline (Fig. 1.6) of the GSL and become "a winter pathway of cold water for the Gulf [of St. Lawrence]" (Galbraith 2006). Table 1.1 is a summary showing estimated inflow magnitudes into the GSL.

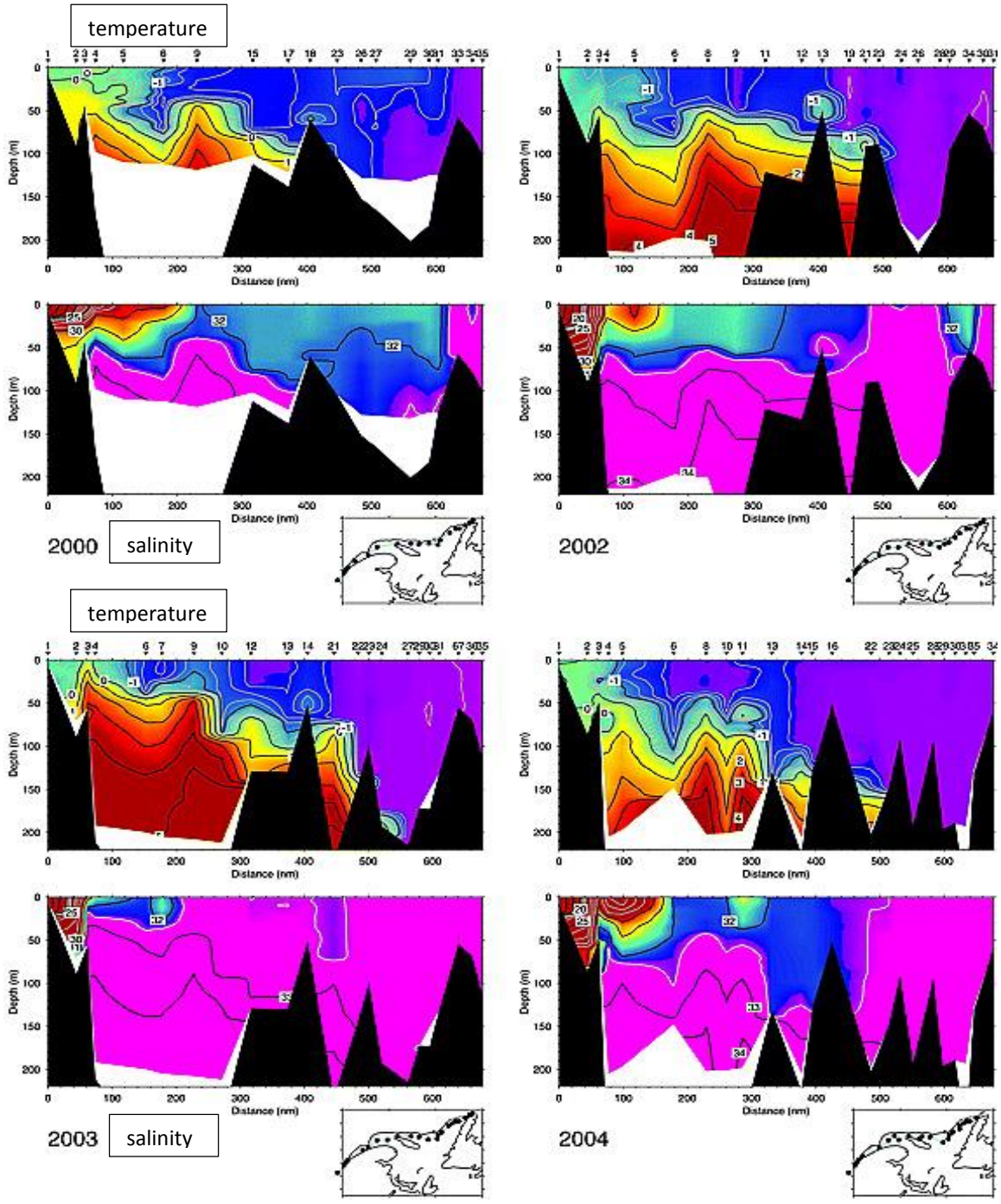

Figure 1.6: Temperature and salinity transects along the northern shore of the GSL from the St. Lawrence estuary to the SBI. Top figure showing temperature, bottom figure showing salinity, white isohaline is 32.35 psu. It shows LC water inflow along northern GSL shore, from Galbraith 2006

Table 1.1. Showing a summary of inflow estimates into the GSL

Location	**Average flow rate/year**	**Source**
Saguenay River & Northern Shore (14% of freshwater in GSL)	1.3 x 10^3 m^3 s^{-1}	Saucier & Chasse (2000)
St. Lawrence estuary (84% freshwater in GSL)	1.9 x 10^4 m^3 s^{-1} 1.1 – 1.7 x 10^4 m^3 s^{-1}	El Sabh (1977) Saucier & Chasse (2000)
Strait of Belle Isle inflow	1.3 x 10^5 m^3 s^{-1} (~31 PSU) 2.2 x 10^5 m^3 s^{-1}	Galbraith (2006), Petrie et al. (1988) Khatiwala et al. (1999)
Cabot Strait inflow	5 x 10^5 m^3 s^{-1} (~34-35PSU)	Khatiwala et al. (1999)

1.4 ICE COVERAGE

The GSL begins to form an ice cover in early January, beginning in the north and west. At the same time, drift ice begins to appear in the northeast through the SBI. By the end of January in situ freezing occurs and about ½ of the GSL is covered with close packed ice, with complete coverage typically occurring by the end of February. Melt begins in early spring, with approximately 50% coverage by March – April, except the extreme northeast where complete coverage persists. It is not uncommon for the SBI to still have 10 - 30 % ice cover in early May. No observational data is available with regards to circulation while ice covers the surface. Trends were observed by tracking the

movement of ice on the surface (Ketchum, 1983). In situ ice formation increases the salinity via brine rejection in the fall, and subsequently the melting in spring adds freshwater. For the scope of this study, the role of sea ice in the fresh water balance was not investigated, but included here to provide a complete description of the GSL.

1.5 Cold Intermediate Layer (CIL)

The cold intermediate layer (CIL) is a cold water mass which is present all year long and is one of the most striking features, even though the precise forming process is still not completely understood. During winter the GSL can be described as a two layer system (Koutitonsky and Bugden, 1991) with a cold but fresh layer overlaying a warmer and saltier bottom layer. From late spring to autumn a three layer system forms when the surface waters warm fast and become fresher while the CIL remain below it. Temperatures in the CIL are close to O℃ year-round with salinity values between 32-33 psu. Beneath the CIL, a warmer water layer (4℃ - 6℃) with salinity of ~34.6 psu consisting of Atlantic water is present. The temperature contrast between the surface layer and the CIL is most pronounced during August, with surface temperatures around 18˚– 20℃ and temperatures only 50 to 60 m below in the CIL remaining close to O˚C. (Gilbert and Pettigrew, 1997). The annual variability of the CIL core temperatures and depth is shown in Figure 1.7 (Gilbert and Pettigrew, 1997). Figure 1.7a shows temperature development of the CIL over the time period of one year.

The number above the error bar represents the number of years used to calculate standard deviation. Figure 1.7b shows depth of the upper (Zi), lower (Zf) 3℃ isotherms as well as the CIL core (Zc) over the time period of one year.

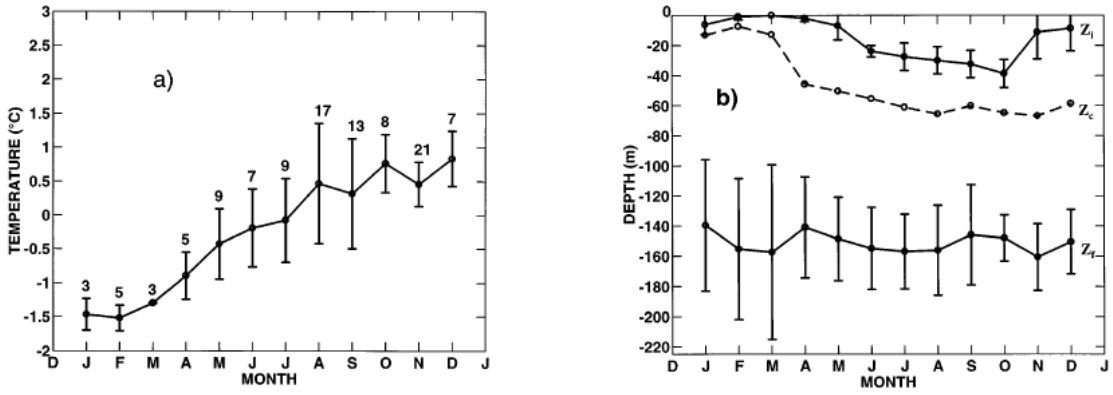

Figure 1.7: From Gilbert and Pettigrew. 1997 a) mean annual cycle of the CIL, defined as waters with T < 3℃ in Northwestern Gulf. b) temperature of core of CIL, Zc and upper and lower 3℃ isotherms, Zi and Zf.

One remaining question is the exact origin of the CIL water masses. Banks (1966) suggested that in situ cooling is the main mechanism for CIL water mass formation and that only 14% of the water forming the CIL is advected through the SBI (T<1.5˚C). Petrie and Toulany (1988) argue that 35% to 53% of the water (having subzero temperatures) enters through the SBI, and therefore the SBI has a greater influence on the formation process of the CIL than the atmospheric forcing; which still plays a role though of less importance. They stated that the waters being forced through the SBI in a given winter form the properties of the CIL the following summer. Smith et al. (2006) believe that their model supports the theory that the CIL is not formed locally, but rather is

advected in through the SBI. When warmer temperatures break the ice cover in the spring, a change in circulation allows the CIL to flow into the estuary from the GSL.

1.6 Forcing mechanisms and general Circulation

Koutitonsky and Bugden (1991) identified four forcing mechanisms acting upon the GSL: The first is buoyancy forcing, driven by the density differences of the different water masses that converge in the GSL: fresh water flowing out of the St. Lawrence Estuary with additional runoff from the northern shore, cold low saline water entering from the SBI, and higher density deep water entering through the Cabot Strait. Bugden (1991) argued that Labrador and Slope waters which enter at depth from the shelf break are advected through the Cabot Strait and affect temperature, salinity and dissolved oxygen content of the water masses in the GSL a few years later. The time lag is explained as a function of the distance from the shelf break up the Laurentian Channel. Budgen (1991), as well as other papers, highlight the estuarine type circulation in the GSL, where a fresher water layer flows seaward on top of a saltier layer, which moves landward (Fig. 1.3).

The mass and freshwater balance in an estuarine system are governed by the following formulas:

Freshwater flux (F) equation:

$$F = \iint_A u \, \frac{S_{ocean} - S_{river}}{S_{ocean}} \, dydz = Q_{river} \quad \text{(Eq. 1.1)}$$

Where S_{ocean} is the ambient ocean salinity value, u is the magnitude of the along channel flow, S_{river} is the local estuarine salinity value of the waters entering the estuary, here from the St. Lawrence estuary system, and Q_{river} is the quantity of the discharged water. A is the cross sectional estuarine area. Since the flux must be constant in the system an increase in S_{river} results in an increase in the integral of u, that is, the net buoyancy current transport.

Mass balance equation:

$$Q_{downstream} = Q_{river} \, \frac{S_{ocean}}{\Delta S} \quad \text{(Eq. 2.1)}$$

$$\text{and} \quad Q_{river} = Q_{downstream} - Q_{upstream} \quad \text{(Eq. 2.2)}$$

Where $Q_{downstream}$ is the quantity of water flowing downstream towards the mouth of the system and $Q_{upstream}$ is the quantity of water coming into the system, and ΔS is the change (difference) between $S_{ocean} - S_{river}$. Equation 2.1 states that the $Q_{downstreams}$ is dependent on the ΔS term. Q_{river} does not change and S_{occean} is stable with no real variation. The only variable that changes is the S_{river} which mixes with ambient, saltier water. By mixing with ambient water the salinity value increases leading to an overall increase of the $\frac{S_{ocean}}{\Delta S}$ term. This change results in a larger $Q_{downstream}$ value. Equation 2.2 states that the total volume of water exiting the system has to equal the amount of water

exiting the river plus the amount of water that is advected in from the ocean. If ΔS decreases it results in a larger $Q_{downstream}$ term, more compensating water ($Q_{upstream}$) has to be advected in to satisfy Equation 2.2

The second forcing mechanism is driven by local and larger regional atmospheric events, which travel along preferred tracks generating costal currents and upwelling of cold water along the northern shore. The third mechanism is tidal forcing from the Atlantic, which produces mixed surface water, internal tides, mixing fronts in coastal areas as well as tidal residuals in the shallow confined areas. For example Wang et al. (1991) described the propagation of internal tides generated at a sill located at the mouth of the St. Lawrence Estuary near where the Saguenay River joins the GSL. The depth at this location is only 25m before it drops to 300m (Laurentian channel). The waters are vertically stratified and the surface tides when flowing over the sill generate an internal tide that propagates seaward. The tidal energy attenuates with downstream distance (Fig.1.8). Wang et al. (1991) concluded that the downstream attenuation is due to a variation in stratification conditions. The fourth mechanism is additional forcing from the Atlantic which generates low frequency perturbations at the edge of the continental shelf. Xu et al. (2013) determined a decadal variation of 3 – 4 Sv stemming from the North Atlantic Oscillation on the sub polar North Atlantic. This large scale oscillation has an effect on the upper and deep LC and a secondary influence on the GSL.

The response to these different forces acting on the GSL produces a general cyclonic circulation in the center of the gulf, where the currents in the channel are dominated by strong cross channel shear with inflow on the southeaster side of the LC and outflow on the southwestern side (Koutitonsky and Bugden 1991, Ketchum 1983).

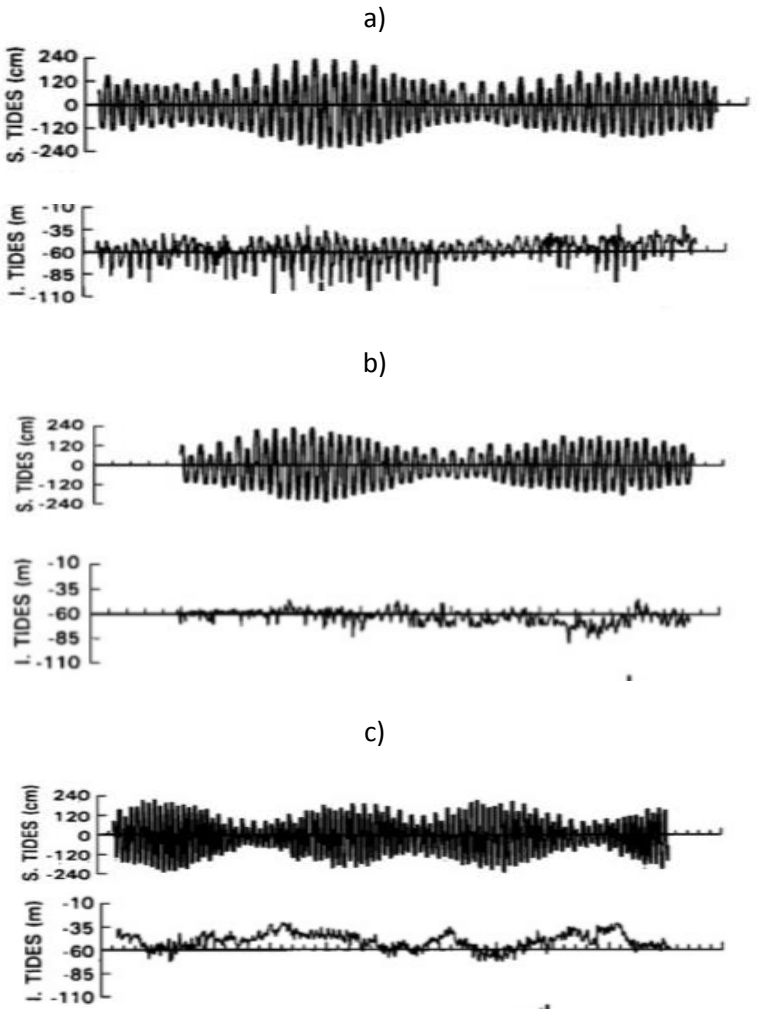

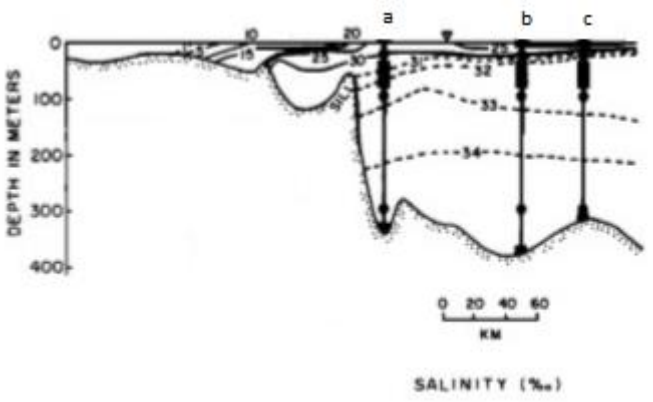

Figure 1.8: Adapted from Wang et al. 1991 showing seaward attenuation of internal tide, locations of measuring station shown in bottom graphic

The inflow magnitude estimates for CS range from 0.45 Sv at the eastern side and outflow at the western side of 0.81 Sv (Saucier et al. 2003) to 0.49 Sv inflow on the eastern side and 0.5 Sv outflow on the western side with a net flow of 0.24 Sv based on mass balance calculations by El Sabh (1977) used by Loder et al. (1998), and to a lesser degree through the SBI.

El Sabh (1977) was the first to identify two year-round features. One is located in the area between the Anticosti Isle and Point de Monts (at the mouth of the St. Lawrence River) where a counterclockwise rotating eddy can be found year-round. Low salinity water exiting the St. Lawrence River meet higher salinity water of the GSL and are mixed (Tang 1980). Though there is a strong annual and inter-annual variability of the currents in the GSL, the Gaspé current is the second persisting year-round feature (Tang, 1980). Fed by the outflow of the St. Lawrence estuary and driven by baroclinic forcing, its surface salinity is 2% lower than surrounding water. The injection of this lighter water into a semi-enclosed area drives a counterclockwise geostrophic flow (Tang 1983). It travels around the Gaspé Peninsula where it is reinforced by a southward current, and along the western coast of the GSL over the Magdalen Shallows finally exiting through the Cabot Strait. Its strength varies with the discharge from the St. Lawrence River, where discharge is stronger in spring and summer and weaker in winter, but its annual mean transport has been calculated by Petrie et al. (1988) to be 0.22 Sv. Figure 1.9 shows overall near surface circulation in summer and winter from a model by Han et al. (1999).

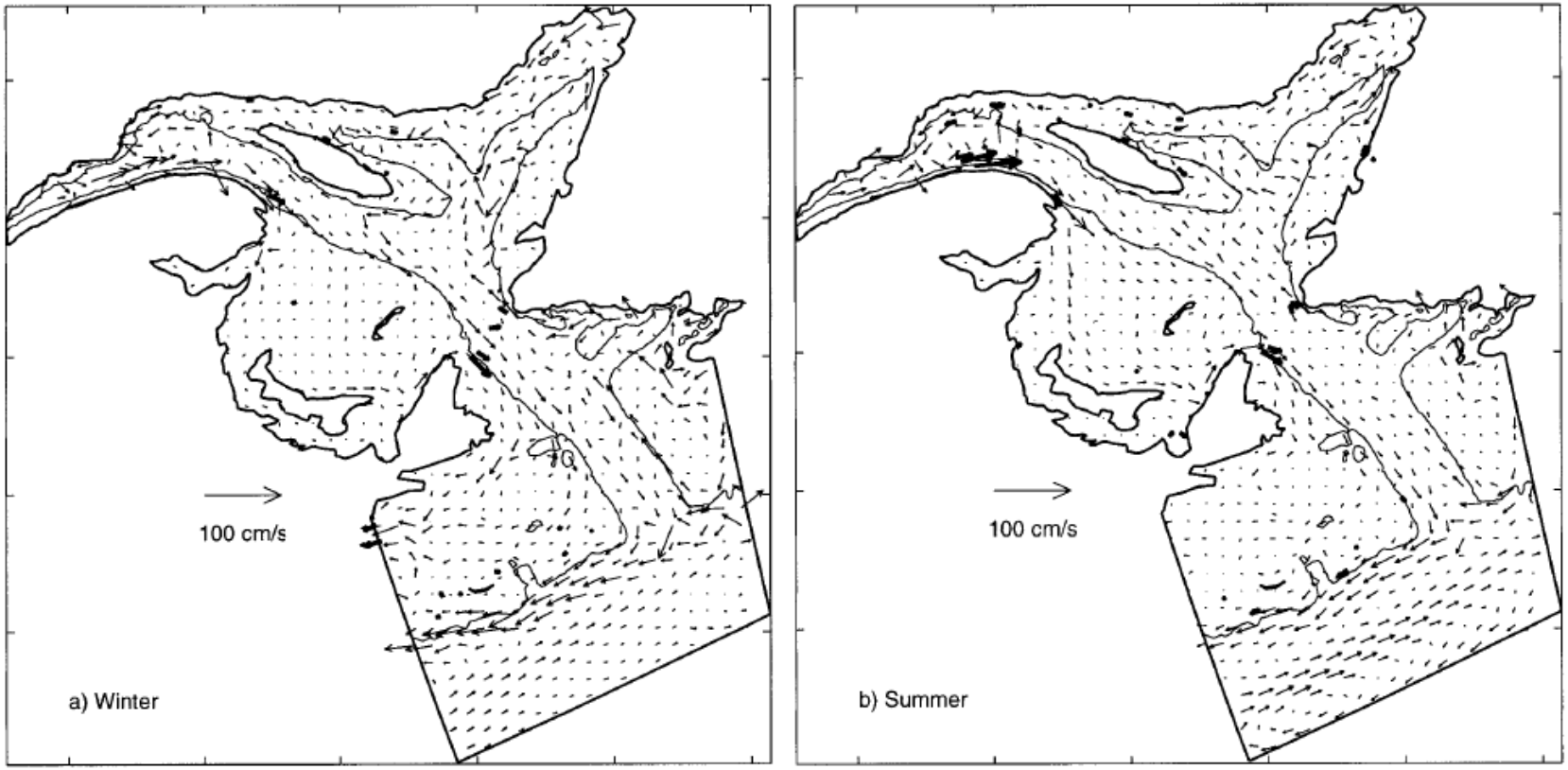

Figure 1.9: From Han et al. 1999 near surface currents 5-30m in a) winter and b) summer. Thin arrows from model solution, thick arrows are observed currents

1.7 IMPORTANCE OF THE GSL OUTFLOW FOR SHELF CIRCULATION

The Labrador Current (LC) is the western bound current in the Labrador Sea, stemming from Greenland and flowing around Newfoundland over the Scotia shelf. It bifurcates and the inshore LC flows up onto the continental shelf entering the GSL through the SBI. The continuing flow on the outer shelf travels around Newfoundland and over the Grand Banks, where its other branch enters the GSL through the east side of the Cabot Strait. It also assimilates the outflow from the GSL (Figure 10 for general circulation of the LC, highlighted areas show in and out flow of GSL). Ohashi and Sheng (2013) revealed that water exiting the St. Lawrence estuary require approximately 100 days to reach the Cabot Strait, 140 days to reach the Scotian Shelf and 220 days to reach the Gulf of Maine. We know that 35% of the freshwater on the continental shelf downstream of the GSL has a $\delta^{18}O$ signature identifying it as originating from the St. Lawrence Estuary (Khatiwala et al. 1999). Downstream of the GSL, the water exiting continues as a buoyancy-driven shelf current further southward along the North American coast carrying cold and relatively fresh waters, forming a boundary between coastal waters and the Gulf Stream. The influence that the exiting water of the GSL has on the western Scotian shelf, as well as further downstream, has been shown in several publications, such as Petri and Drinkwater (1993) and Han et al. (1997, 1999). Drinkwater and Gilbert (2004), show that the relatively fresh water that exit the GSL seasonally shifts towards the ocean (Fig. 1.10). Although outflow occurs year-round, the maximum/minimum outflow occurs in the fall/spring (Han and Loder 2003). This seasonality is related to freshwater discharge of the St. Lawrence estuary system.

Figure 1.10 shows surface isohaline being pushed seaward and driven by increased freshwater discharge of the St. Lawrence River. The 31 psu isohaline is the most indicative and depicts the expansion of the freshwater plume in summer moving further onto the shelf, while in the winter it stays close to shore turning right (in flow direction) after exiting the GSL. Loder et al. (1998) identified that sub-polar water on the shelf and further downstream stem from the Labrador Current and is seasonally enhanced by the CS outflow. They also identified three sources for freshwater on the Northeastern north American shelf as 1) the Labrador current 2) GSL runoff 3) ice melting, in this order of magnitude. The outflow also drives cross shelf transport through channels and gullies running across the shelf, connecting the shelf with nutrient rich Atlantic waters, effecting biology on the shelf as well as in the GSL (Drinkwater and Gilbert 2004).

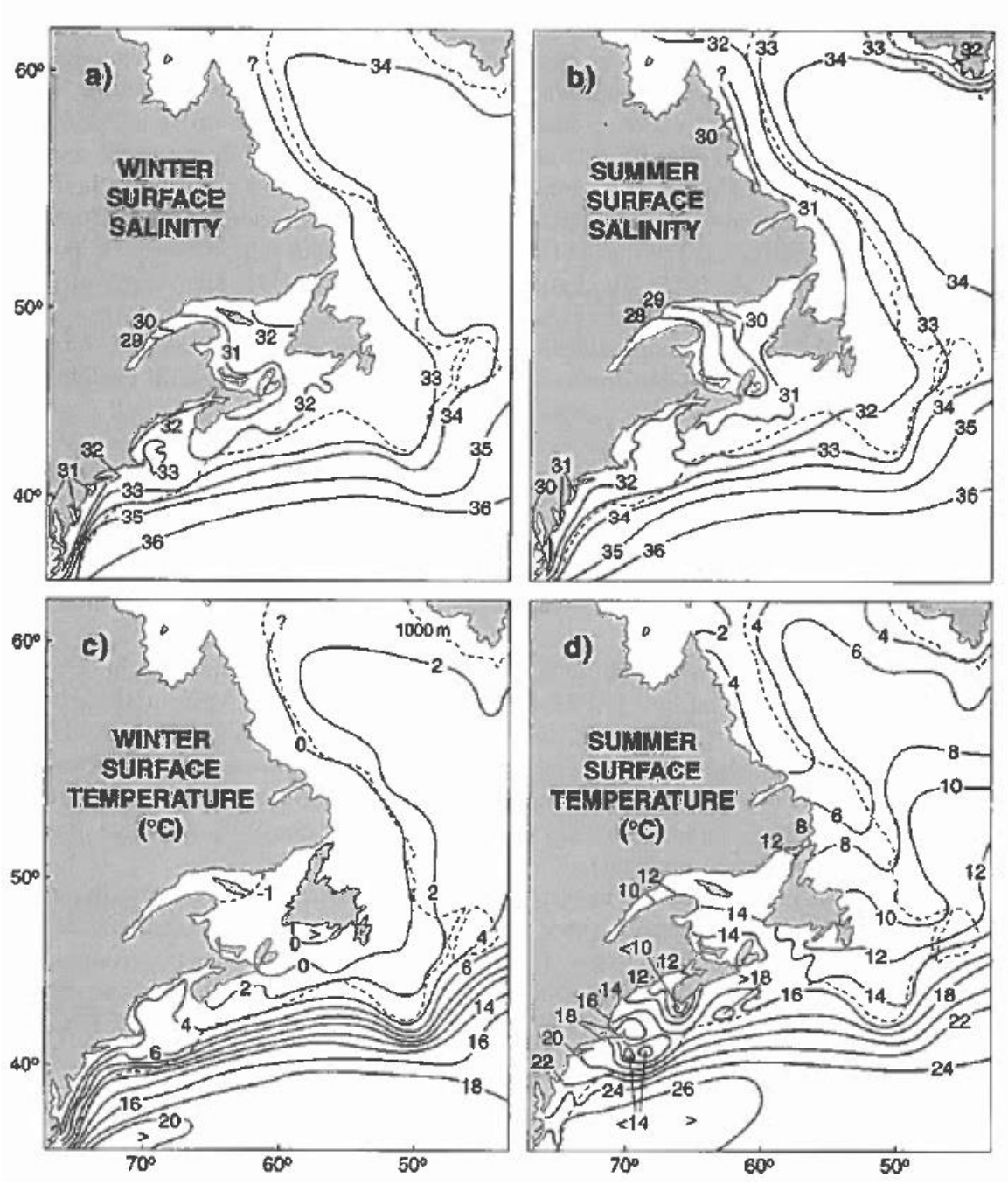

Figure 1.10: From Loder et al. 1998 depicting salinity and temperature in winter and summer

CHAPTER 2 DATA PROCESSING AND ANALYSIS

2.1 HYDROGRAPHIC DATA SELECTION AND SCREENING

A climatology depicts the average state of a system over a chosen time period, or per Linder and Gawarkiewicz (1998): "Climatologies are useful in describing the 'mean' conditions". The data used for our analysis comes from hydrographic stations and were provided by NOAAs National Oceanographic Data Center (NODC). We selected 3 locations for our vertical transects, so that the St. Lawrence River discharge to the GSL as well as the in and out-flow through the CS are captured at the surface and at depth, for us to better record the perceived estuarine type circulation. This area best represents where the dominant estuarine regime occurs. The locations were named Cabot Strait (CS) Anticosti (AC) and Strait of Belle Isle (SBI) (Fig. 2.1). After a preliminary analysis of the data we decided to narrow the time window for our analysis to 60 years from 1950 to 2010, due to the availability of consistent data, and we selected ice free months from May through October when the St. Lawrence discharge is large and buoyancy forcing dominates. This time frame also allowed us to filter out inter-decadal and most of multi-decadal natural climate oscillations, with the exception of the Atlantic Multidecadal Oscillation, which shows a variability of 60 – 75 years (Skliris et al. 2014).

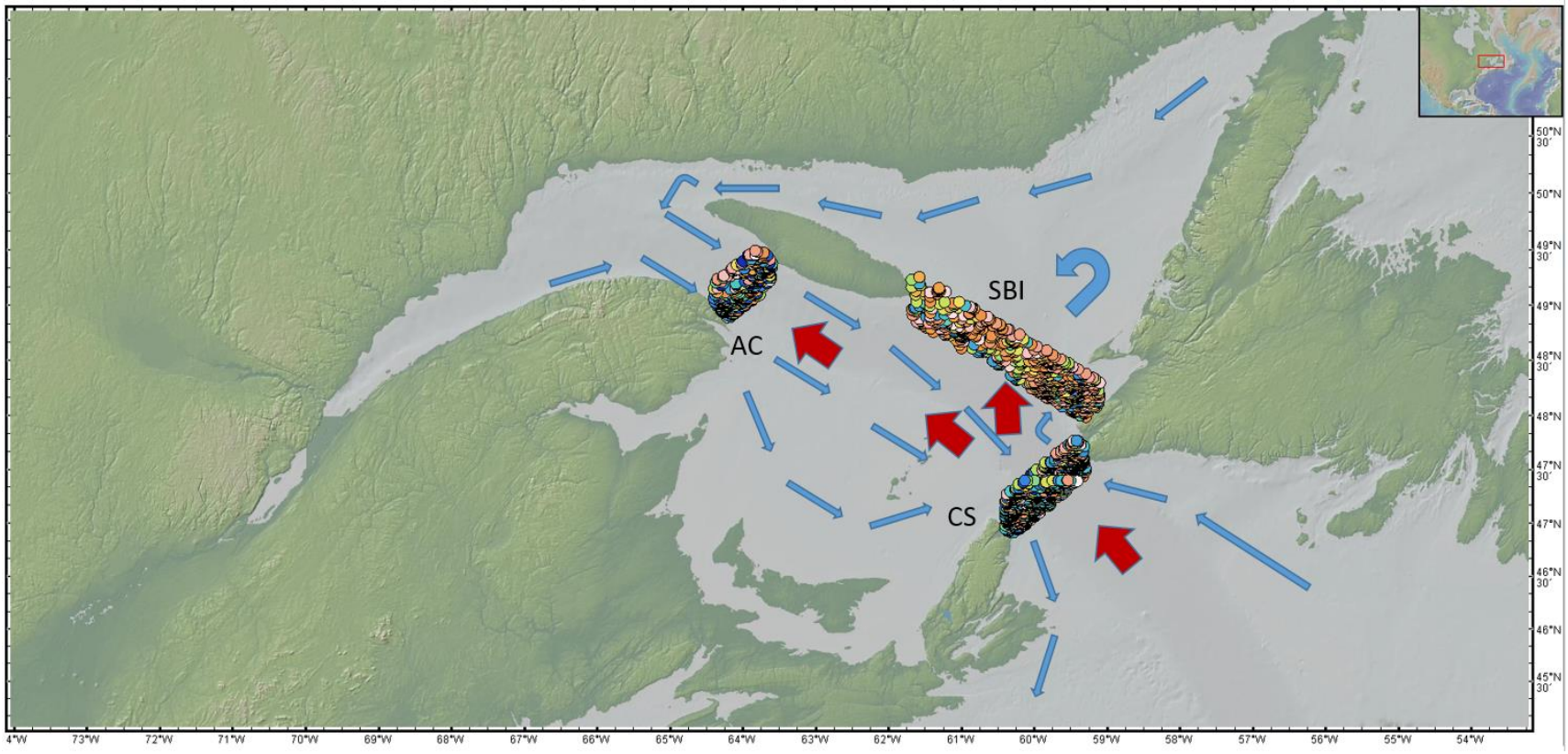

Figure 2.1: Location of hydrographic stations used; Cabot Strait (CS), Anticosti (AC), Strait of Belle Isle (SBI), with schematic water flows. Arrows represent pathways for circulation in the upper layer (blue), and in the deep layer (red). Adapted from GeoMapApp http://www.geomapapp.org

All sorting, data manipulations and averaging was done with Matlab®. Quality control was automated and underwent additional visual inspection. Each transect had a width of 50km (along channel). Each station had to have a minimum of three measure points to be included in the climatology. We applied a filter to find multiple recordings of the same casts (using individual cast numbers) and kept only one record if duplicate casts were detected. A script was run removing stations with values outside of three standard deviations from the mean (Fig.2.2).

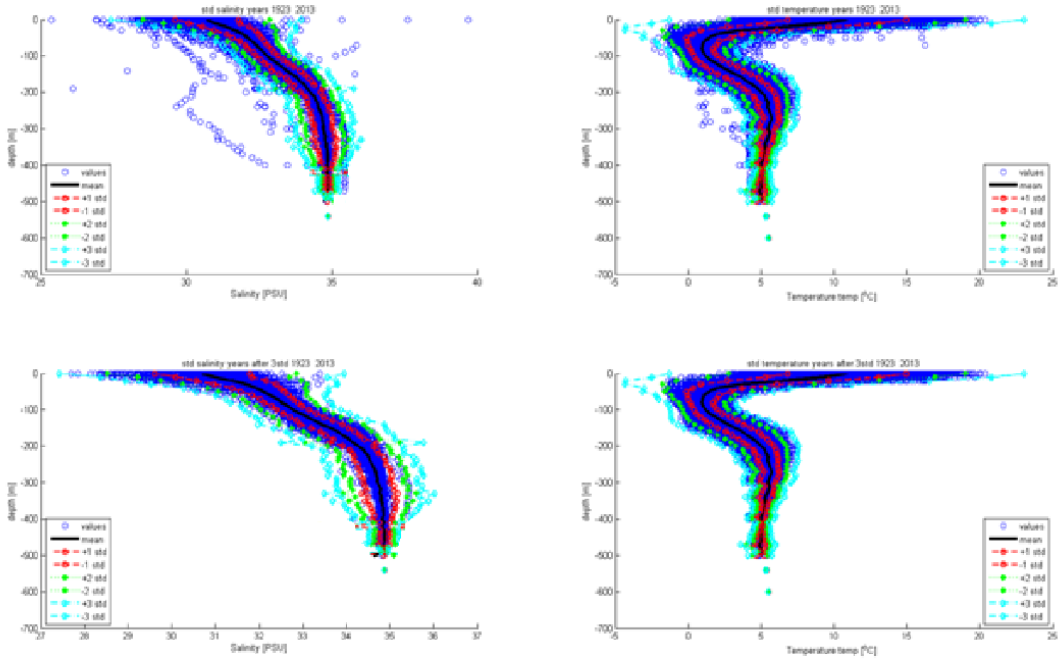

Figure 2.2: Top row shows data before sorting out values larger than 3 standard deviations, bottom row shows data after removing values larger than 3 standard deviations. Left column is salinity, right column temperature

A linear interpolation for each station was conducted, with a vertical bin size of 5 meters, the deepest measuring point also being the last point; no extrapolation was conducted. The data were then visually inspected, and stations that had a maximum depth

exceeding what was physically possible for the selected area, were manually removed. The same method was used to remove stations in impossible locations, such as being on islands. We suspect that when the database was compiled some stations must have been entered with incorrect latitude and longitude values, which led to impossible depths (for example +1000 m within the GSL or coordinates that locates them on an island or on/very close to shore with a depth of +200m).

2.2 CLIMATOLOGICAL TRANSECTS AND THEIR SUBDIVISION

After the data passed quality control, climatological fields were estimated. The transects were subdivided into grid cells with 10m depth, 10km length (cross channel) and 50km width (along channel) . The mean of temperature and salinity was taken for every grid cell to construct an overall climatology (Fig. 2.3 a b) for the complete ice free time period referred to as semi-annually (May – October).

Figure 2.3a shows the stratification in the GSL. The CIL for example can be easily distinguished in figure 2.3b, displaying the lowest temperature in the middle of the figure. Also the freshwater discharge from the St. Lawrence River in the top left corner of figure 2.3a can easily be distinguished. The isohalines slopes are steeper depicting the freshwater inflow. In figure 2.3b we can see the warmer waters spread across the surface layer.

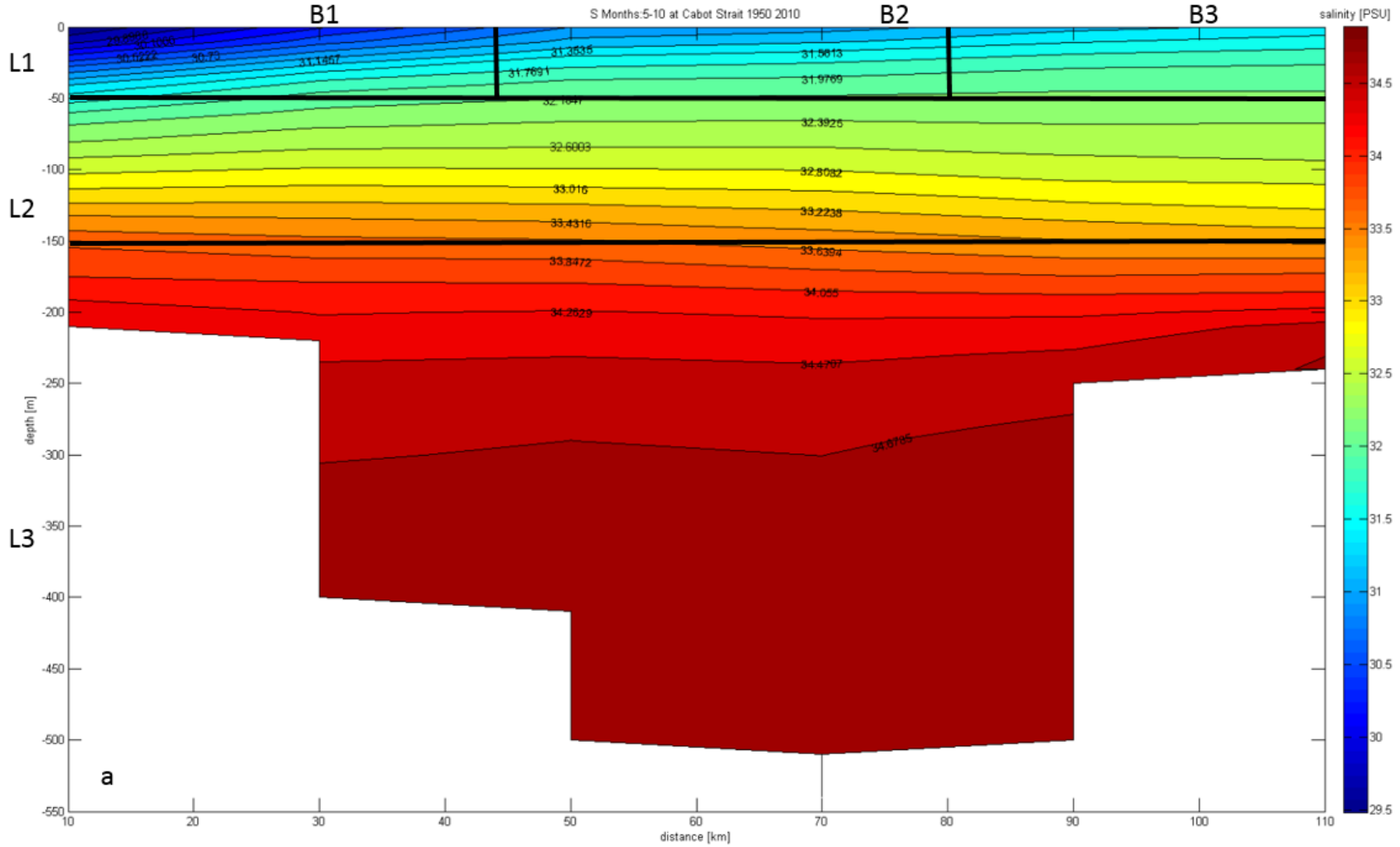
B1
S Months:5-10 at Cabot Strait 1950 2010
B2
B3
salinity [PSU]
L1
L2
L3
depth [m]
distance [km]
a
31.1467
31.3535
31.5613
31.7691
31.9769
32.1847
32.3925
32.6003
32.8082
33.016
33.2238
33.4316
33.6394
33.8472
34.055
34.2629
34.4707
34.6785

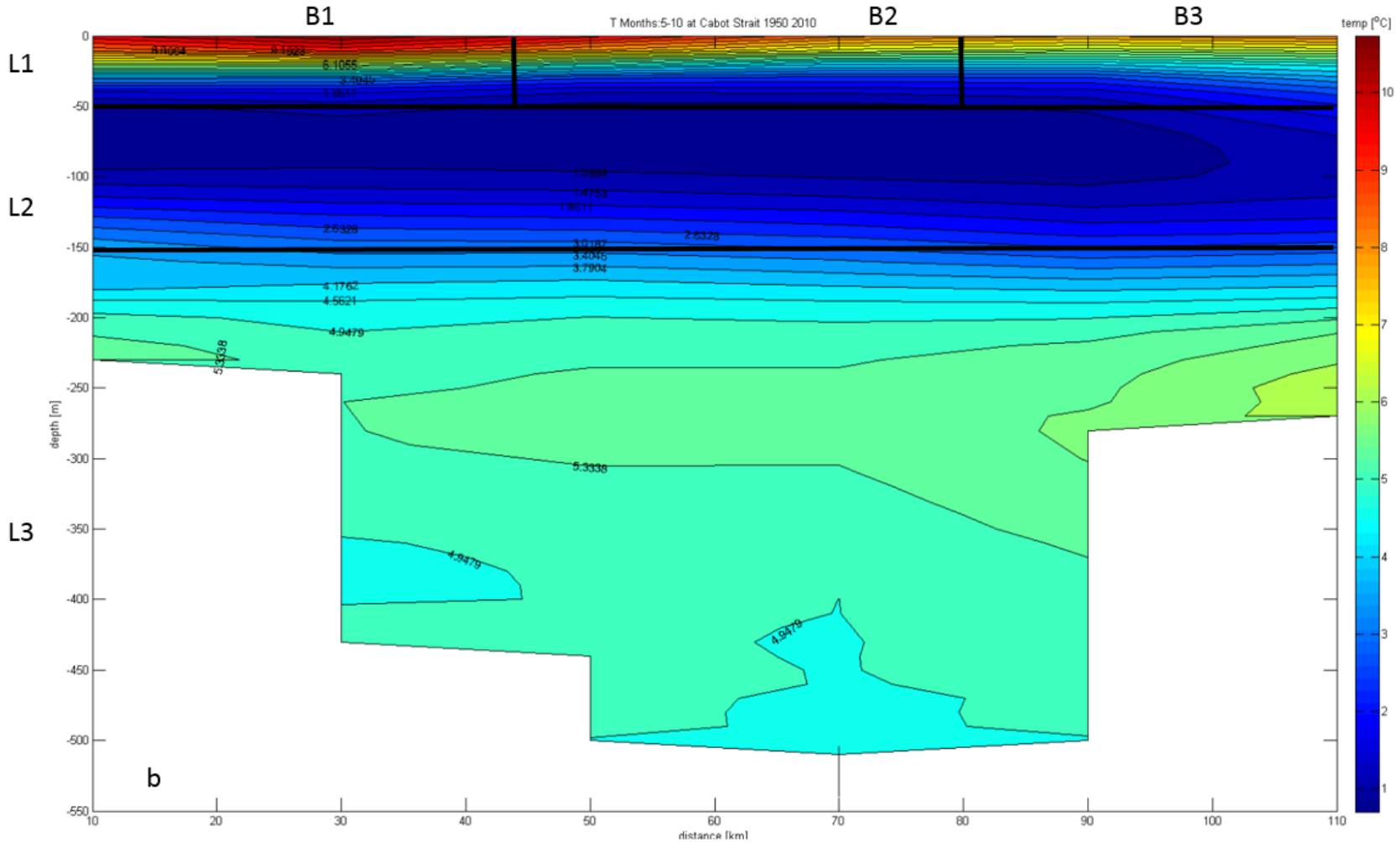

Figure 2.3 a b: CS climatology for salinity (a) and temperature (b) for CS

It is the warmest where the freshwater is discharged from the St. Lawrence River, creating a temperature gradient from west to east. Figure 2.4 a and b show the standard deviation from the mean (temperature and salinity respectively); areas with little change through the seasons have a low standard deviation indicating the center (stable area) of the water mass, while areas with high variability depict boundary areas between 2 layers (area with high rate of change). For example figure 2.4 a confirms the inflow of freshwater to the system to be in the top left corner where it shows a high variability for salinity. This variability is due to the change of the flow magnitude throughout the year. The temperature and salinity figures in combination with the standard deviation figures were used to properly define the three layers. A surface layer corresponds to the seasonal thermocline with highly variable temperature and salinity due to its exposure to the atmospheric conditions, freshwater influxes and strong mixing regime (L1), 0-50m at CS and AC, and 0-25m at SBI. The CIL has relatively stable temperatures around 0°C and salinity values around 32-33 psu (L2), 50-150m for CS and AC, and 25-200m at SBI. A deep layer made up of Atlantic water entering the GSL at depth with temperatures of 4-6°C and a salinity ~ 34.6 psu (Smith et al. 2006) (L3), 150-550m at CS, 150-400m at AC and 200-450m at SBI. We then subdivided the L1 into 3 Boxes (B1, B2, B3) for CS and 2 Boxes (B1, B2) for AC. Boxes 1 on both transects are occupied by the buoyance driven current from the St. Lawrence River. Box 2 at AC and Box 3 at CS are dominated by the LC waters.

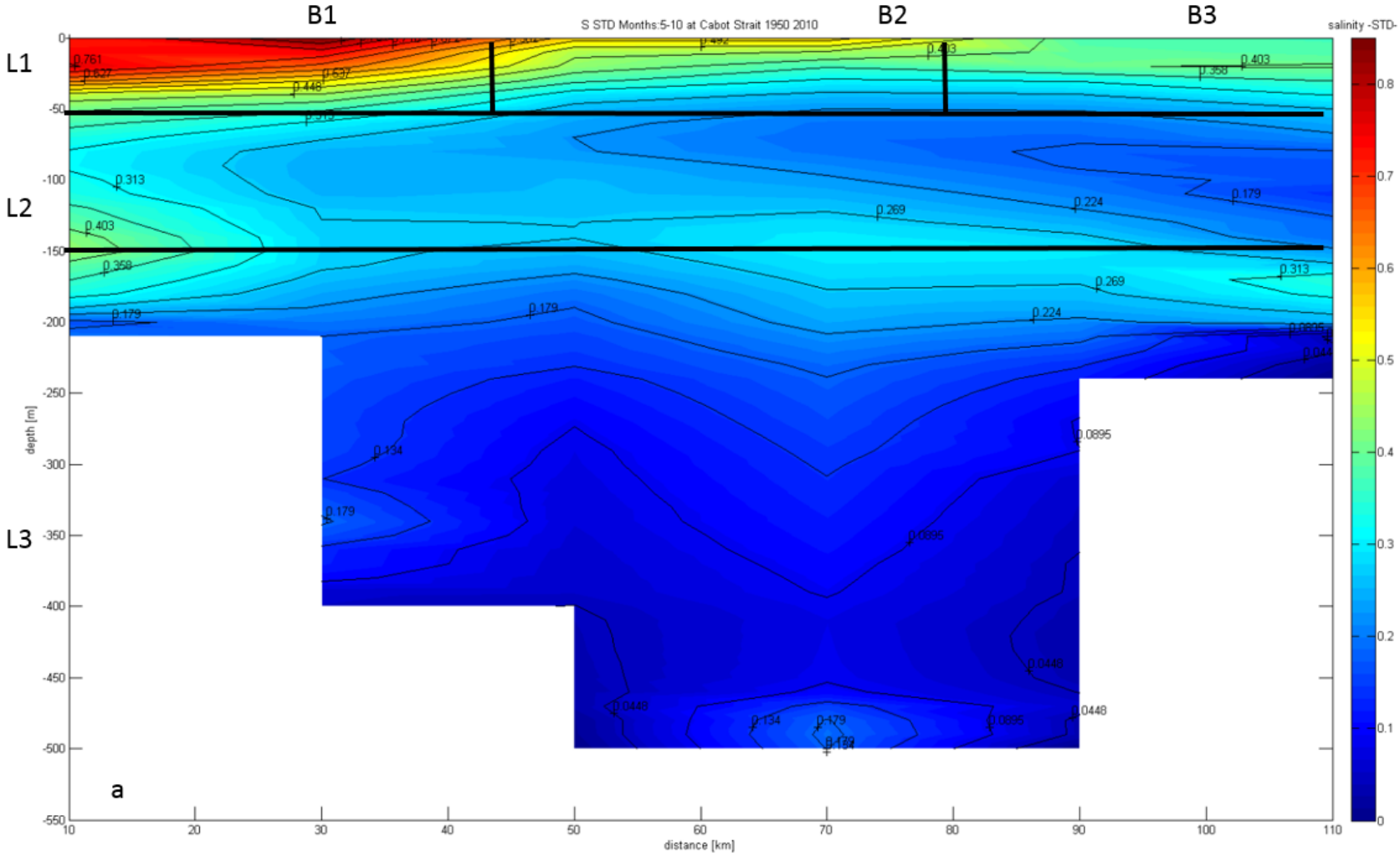
B1
B2
B3
S STD Months:5-10 at Cabot Strait 1950 2010
salinity -STD-
L1
L2
L3
depth [m]
distance [km]
a

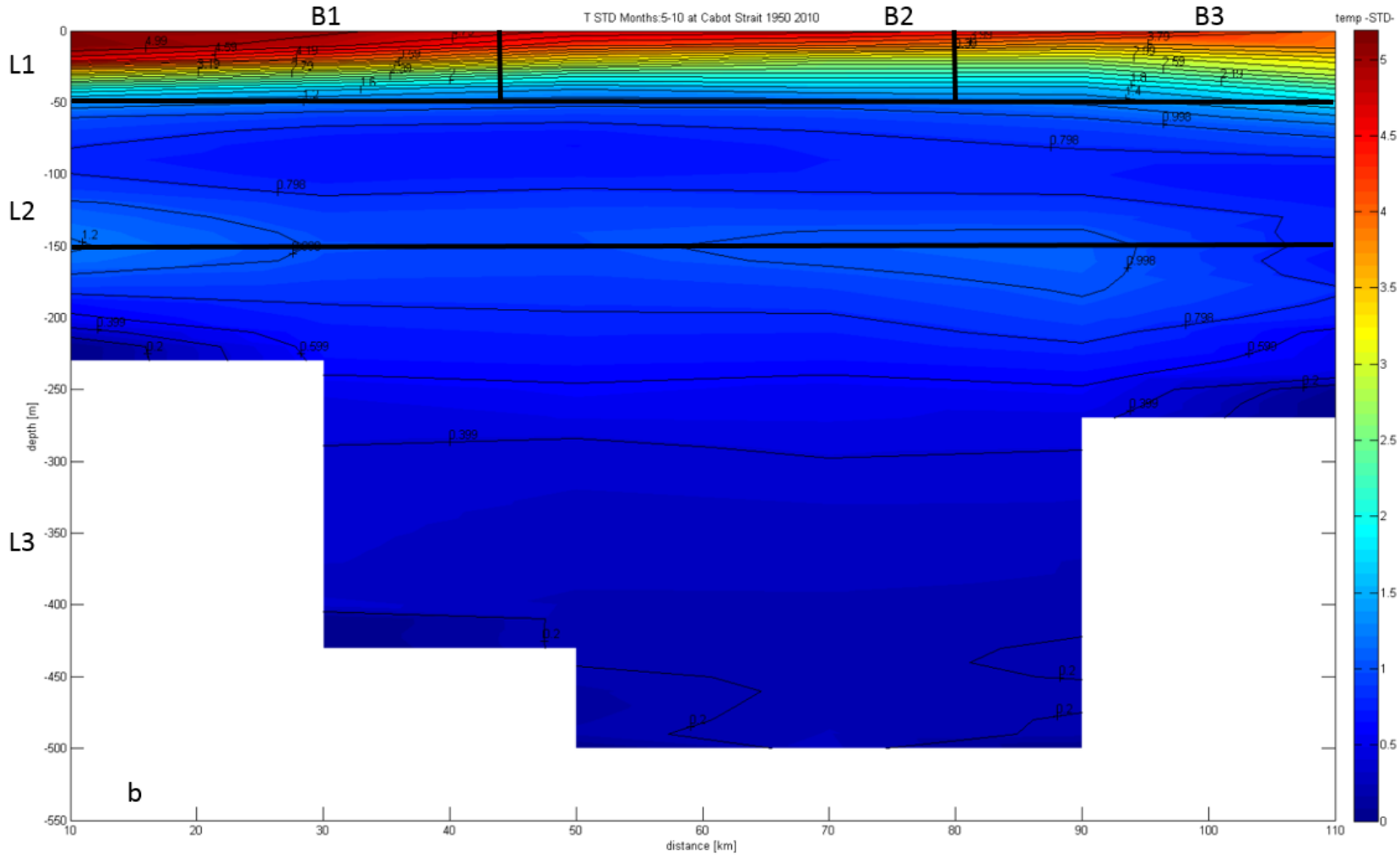

Figure 2.4 a b: CS standard deviations of salinity (a) and temperature (b)

2.3 TEMPORAL EVOLUTION OF ANNUAL ANOMALIES

The data for each layer and box were then averaged and reduced to one annual value (yearly mean) and plotted with a 95% confidence interval as well as the linear least squares fit line and slope thereof. This was done for each two-month interval (5-6, 7-8, 9-10), as well as for the whole timeframe (5-10) (Fig. 2.5 a b).

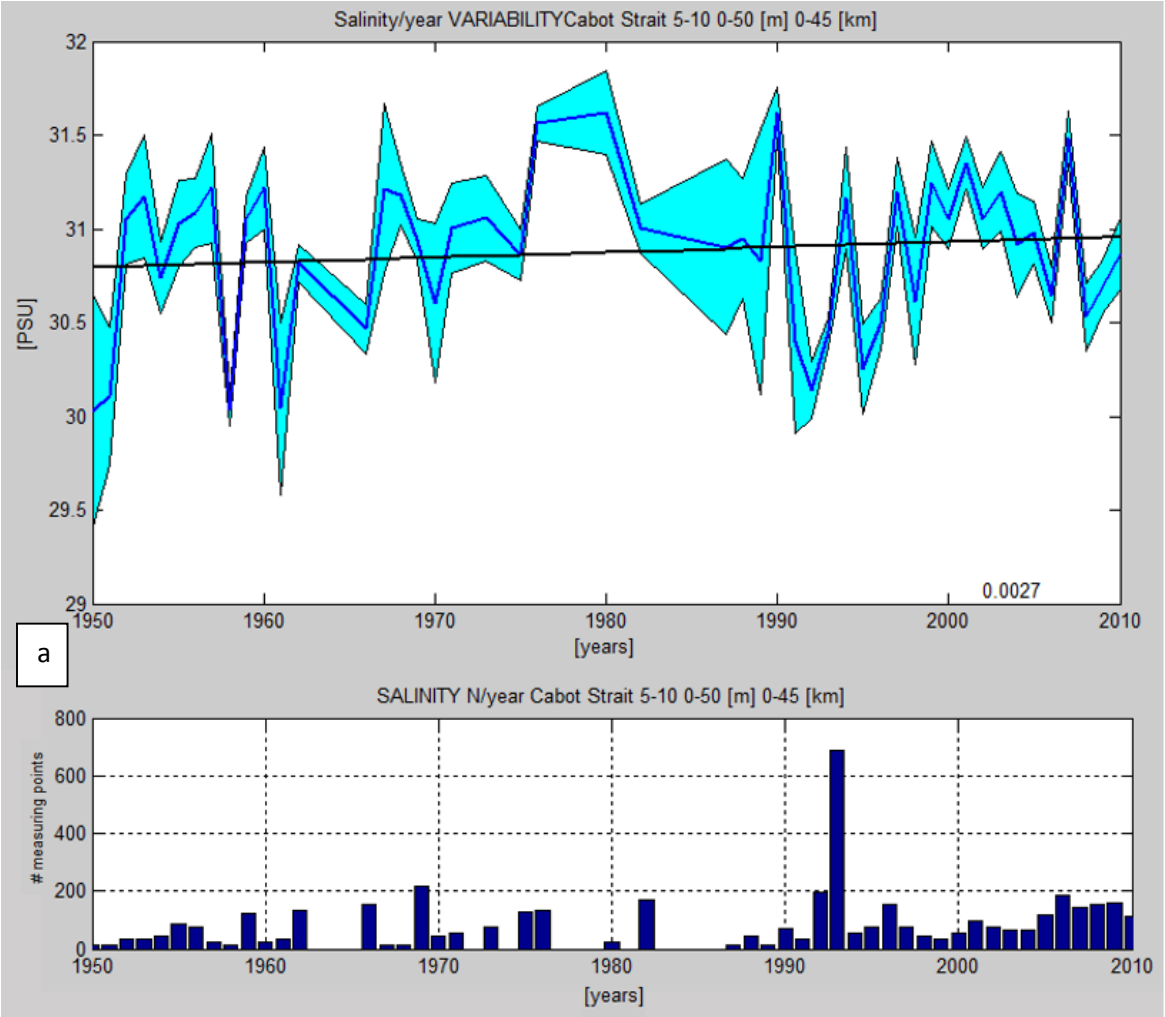

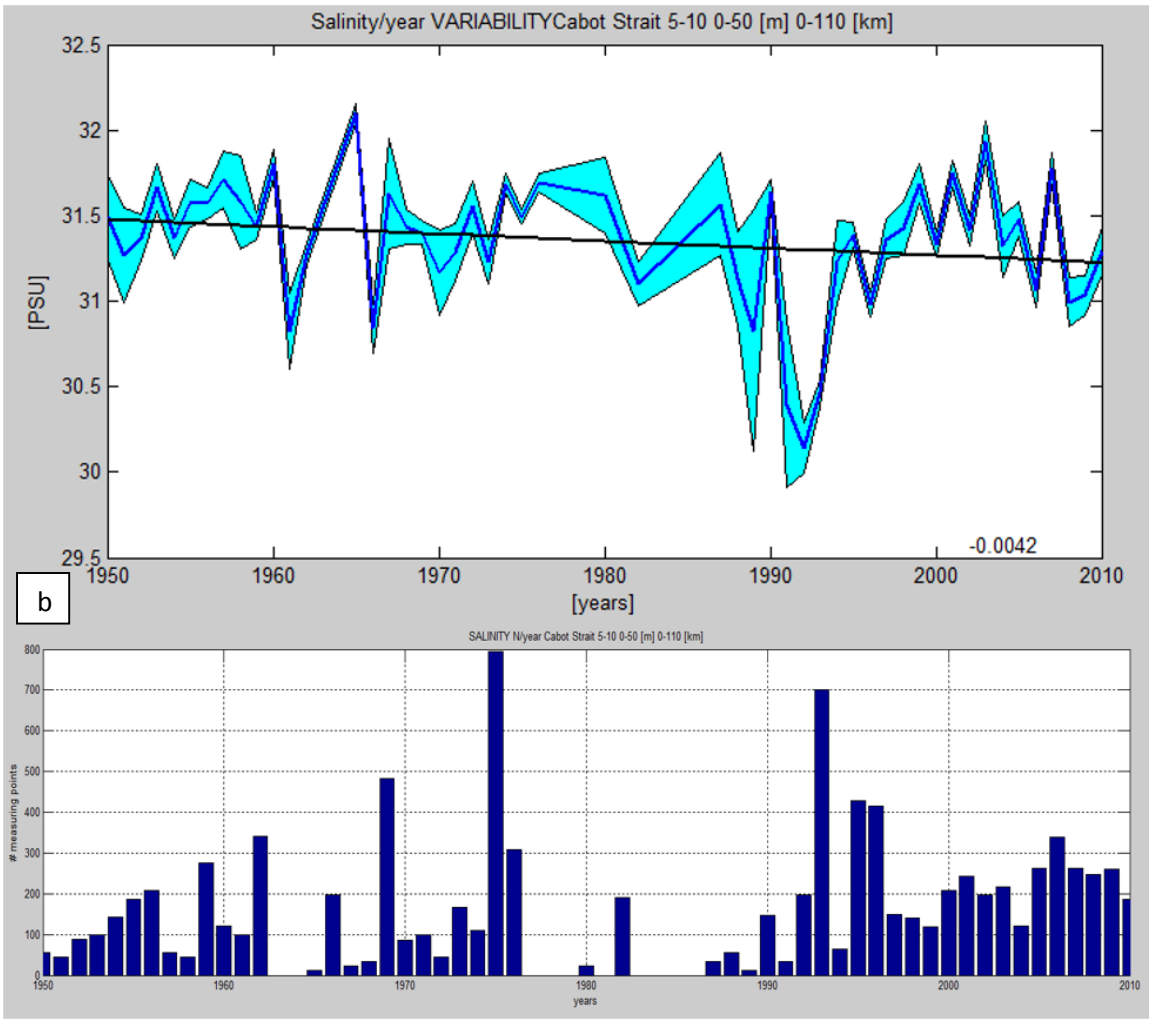

Figure 2.5: a b are example for salinity yearly value with 95% c.i., least square line and slope. Figure 2.5 (a) depicts box one at CS. Figure 2.5 (b) depicts layer one at CS. Both show temporal distribution and amount of measurement points/year.

We subtracted the climatology from the annual values to determine the anomalies. This was done for bi-monthly and semi-annual values. Semi-annual means that values for the entire time frame (5-10) were averaged. Some discrepancies exist between the semi-annual and bi-monthly results. This stems from when individual casts were made. Not all years have been sampled evenly throughout every three bi-monthly time period. Some years where not sampled at all. A bias occurred when samples were only (or almost exclusively) taken in one bi-monthly period, such that the year displays a bias toward said period. If the samples were predominantly taken during the first bi-monthly period for example the whole year would be showing colder temperatures. In addition the time period from the early 1970s until mid-1980s has generally been under sampled, resulting in data gaps. If the measurements were distributed more evenly throughout the year a more consistent picture would have emerged. To counteract the non-uniform distribution of the sample points we applied a similar method similar to that employed by Drinkwater and Gilbert, 2004 and Skliris et al., 2014. Once the bi-monthly mean for the entire time series was established, we averaged each year into three bi-monthly values, and subtracted the bi-monthly overall mean from corresponding yearly mean for the same bi-monthly time frame. The three resulting anomaly values were then averaged resulting in one yearly anomaly value. Figure 2.2 a and b shows the discrepancy between the bi-monthly averaged anomalies and the semi-annual anomalies. Figure 2.6 a shows salinity for CS layer one, where both methods show a close fit and almost identical slopes for the two least square lines. Figure 2.6 b shows temperature for AC box 2, with the largest discrepancy. The difference between the slopes is -0.0003 which is one order of magnitude smaller than the leading order trend. In the upper panel we can see the bias

towards more extreme anomalies using the semi-annual method versus the bi-monthly method.

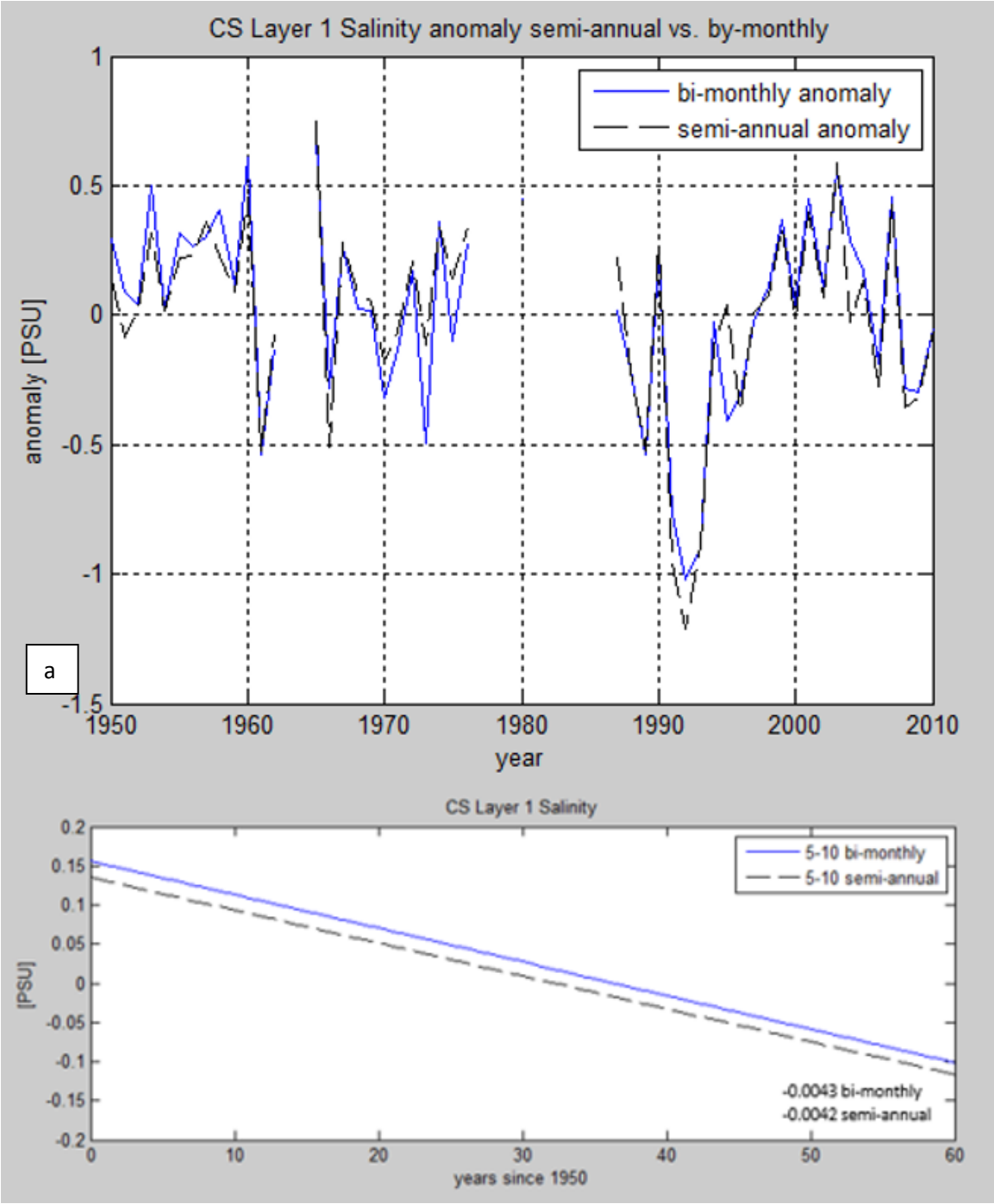

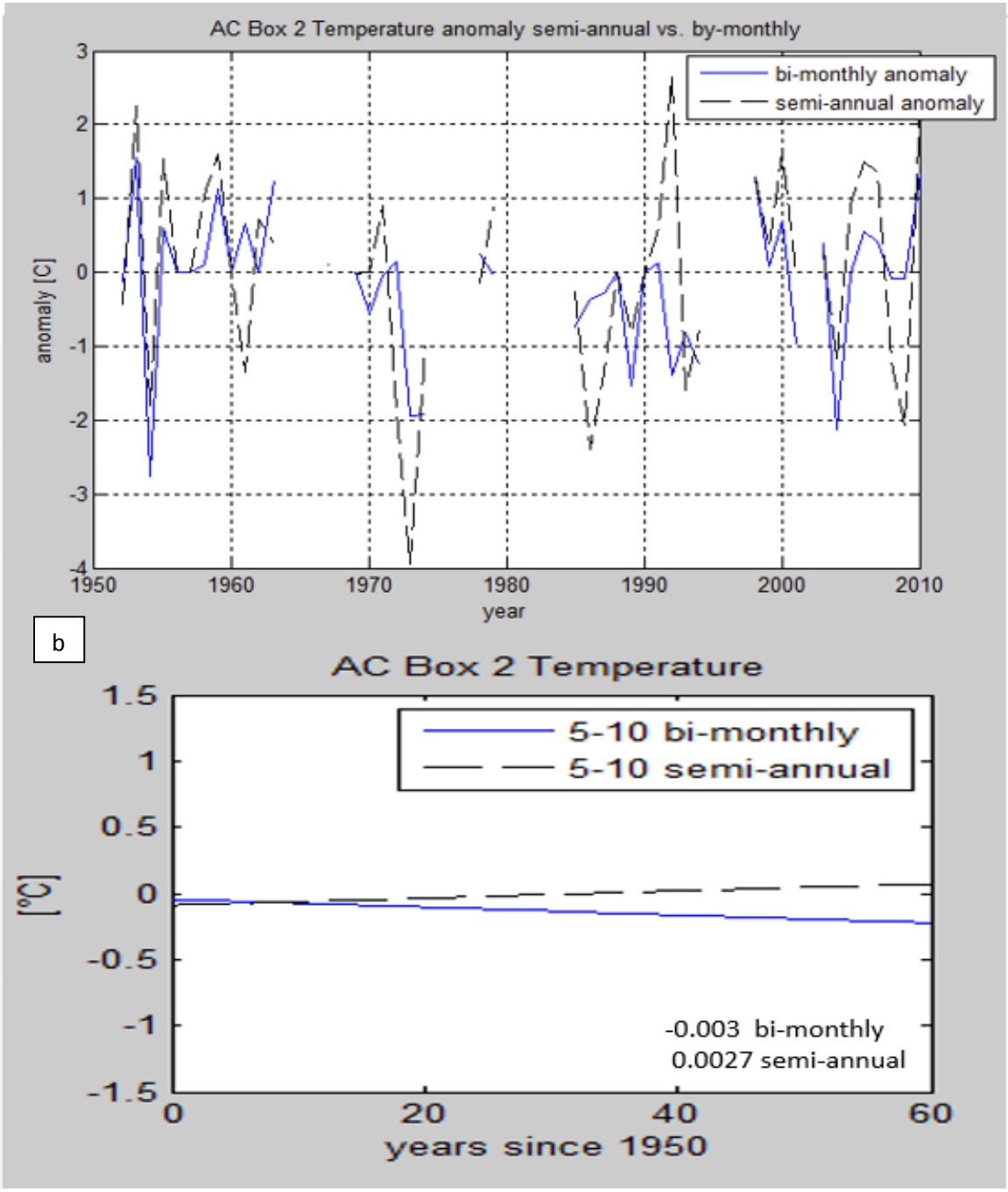

Figure 2.6: Bi-monthly and semi-annual salinity 2.6 (a) and temperature 2.6 anomalies (b) with least squares fit line 2.6 a showing good agreement between bi-monthly and semi-annual anomaly, 2.6 b showing largest discrepancy between bi-monthly and semi-annual anomaly.

Fig 2.7 is an example showing CS layer one, two and three, salinity and temperature least squares linear fits and corresponding trends. Hereinafter, we only used the non bias bi-monthly values from this point on for all analyses.

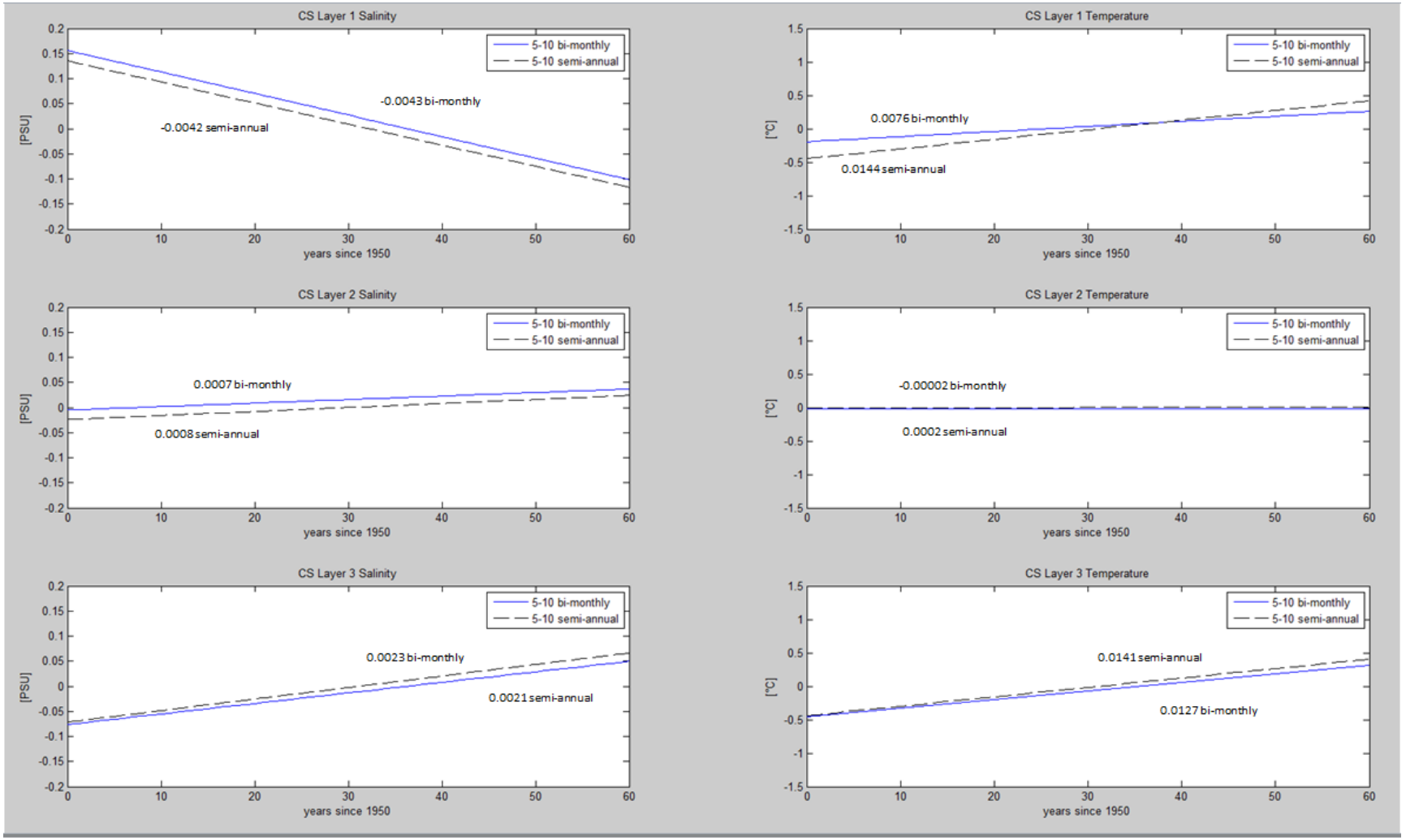

Figure 2.7: Selected final least squares lines and slopes for CS all Layers

CHAPTER 3: SUMMARY AND DISCUSSION

3.1 DOMINANT TRENDS IN HYDROGRAPHIC CLIMATOLOGY

Table 3.1, 3.2 and 3.3 summarize the climatological trends of our study for the different boxes and layers. A positive/negative (red/blue) trend for temperature indicates a warming/cooling and a salting/freshening for salinity. From all the trends we defined the largest order of magnitude to be the leading order trends, which are 10^{-2} for temperature and 10^{-3} for salinity. Values at this order of magnitude are considered substantial. Substantial trends are in displayed in bold.

Table 3.1: results showing trend for temperature/salinity at CS.

Cabot Strait 5--10		bi-monthly
Box 1	Temperature	-0.0013
0-50m 0-45km	Salinity	**0.0038**
Box 2	Temperature	0.0076
0-50m 45-80km	Salinity	-0.0002
Box 3	Temperature	**0.0126**
0-50m 80-110km	Salinity	**-0.0012**
Layer 1	Temperature	0.0076
0-50m 0-110km	Salinity	**-0.0043**
Layer 2	Temperature	-0.00002
50-150m 0-110km	Salinity	0.0007
Layer 3	Temperature	**0.0127**
150-550m 0-110km	Salinity	**0.0021**

Table 3.2: results showing trend for temperature/salinity at AC

Anticosti 5--10		bi-monthly
Box 1	Temperature	**-0.0255**
0-50m 0-40km	Salinity	**0.0033**
Box 2	Temperature	-0.003
0-50m 40-80km	Salinity	**-0.001**
Layer 1	Temperature	**-0.0174**
0-50m 0-80km	Salinity	-0.0009
Layer 2	Temperature	-0.0049
50-150m 0-80km	Salinity	**0.0018**
Layer 3	Temperature	**0.0174**
150-400m 0-80km	Salinity	**0.0046**

Table 3.3: results showing trend for temperature/salinity at SBI.

Strait of Belle Isle 5--10		bi-monthly
Layer 1	Temperature	**0.0122**
0-25m 0-221km	Salinity	-0.0003
Layer 2	Temperature	**-0.0104**
25-200m 0-221km	Salinity	**0.0027**
Layer 3	Temperature	0.00134
200-450m 0-221km	Salinity	**0.0017**

L1 exhibits the most variability between transects, which was to be expected since it encompasses both local buoyancy forcing and water fed by non-local forcing. CS shows a non-substantial warming (0.0076) and a substantial freshening (-0043) trend. Looking closer at the different boxes in the CS we see B1, dominated by the buoyancy driven outflow from the St. Lawrence river, to show a non-substantial cooling (-0.0013) and substantial salting (0.0038) trend. B2 which is influenced by both the LC and periodically, when large freshwater pulses expand the freshwater plume, by the buoyance driven outflow. It remains relatively steady with a non-substantial warming (0.0076) and freshening (-0.0002). B3, which is influenced by the LC, shows a substantial warming (.0126) as well as a substantial freshening (-0.012) trend.

AC surface layer shows substantial cooling (-0.0174) and non-substantial freshening (-0.0009). B1, dominated by the buoyancy driven outflow of the St. Lawrence River, shows substantial cooling (-0.0255) and salting (0.0033) trends, while B2, which is under the LC influence has a non-substantial cooling (-0.003) and borderline substantial freshening (-0.001). SBI L1, which is dominated by the LC waters entering the CS at the surface, has a substantial warming (0.0122) but a non-substantial cooling (-0.0003) trend.

L2 also exhibits an overall cooling and salting trend at all locations. At CS both temperature (-0.00002) and salinity (0.0007) are below the leading order trend. AC has a temperature (-0.0049) below the leading order trend but the salinity (0.0018) is of the leading order trend, while SBIs temperature (-0.0104) and salinity (0.0027) are both substantial (larger than leading order trend).

All three transects show a substantial trend towards warming and salting in L3 with the exception of the SBI which shows a warming trend one order of magnitude smaller than the leading order trend (0.00134). L2 and L3 are both relatively stable layers and their behavior is consistent at all transects which is reflected in our results.

3.2 DISCUSSION:

We looked at discharge of the St. Lawrence River from 1955 to 2010. The data was provided by the St. Lawrence Global Observatory. It consists of measurements taken at a flow gauge at Quebec City, and uses Bourgault and Koutitonsky (1999) freshwater runoff model to complete missing data. Figure 3.1 suggests a tendency for slight increase in runoff over the considered time interval. Bourgault and Koutitonsky (1998) demonstrated an inter-decadal variability, which is reflected in our findings. In addition if we look at the discharge from 1974 until 2010 we can estimate a negative slope, meaning a decreasing trend in runoff. Long-term predictions estimate that runoff will decrease due to climate change. Mortsch and Quinn (1996) ran a simulation doubling 1996 CO^2 regime, and concluded that the runoff from the Great Lakes would be reduced by 40% under those conditions. Such a drastic decrease in runoff would change the buoyancy forcing in the GSL. For the scope of this study we assume that the discharge rate is nearly constant, although we believe that in the near future a decrease in overall discharge will occur. We also plotted salinity anomaly against the runoff for CS and found no significant correlation. R2 values were 0.0046 for box one, 0.1333 for box two and 0.1516 for box three (Fig 3.2 a, b, c). The linear regression lines are in accordance with out hypothesis that increased runoff in the buoyance driven current (box 1) brings

(through increased mixing) an increase in the volumetric transport of the compensating deep water inflow. This response is governed by the balance equations.

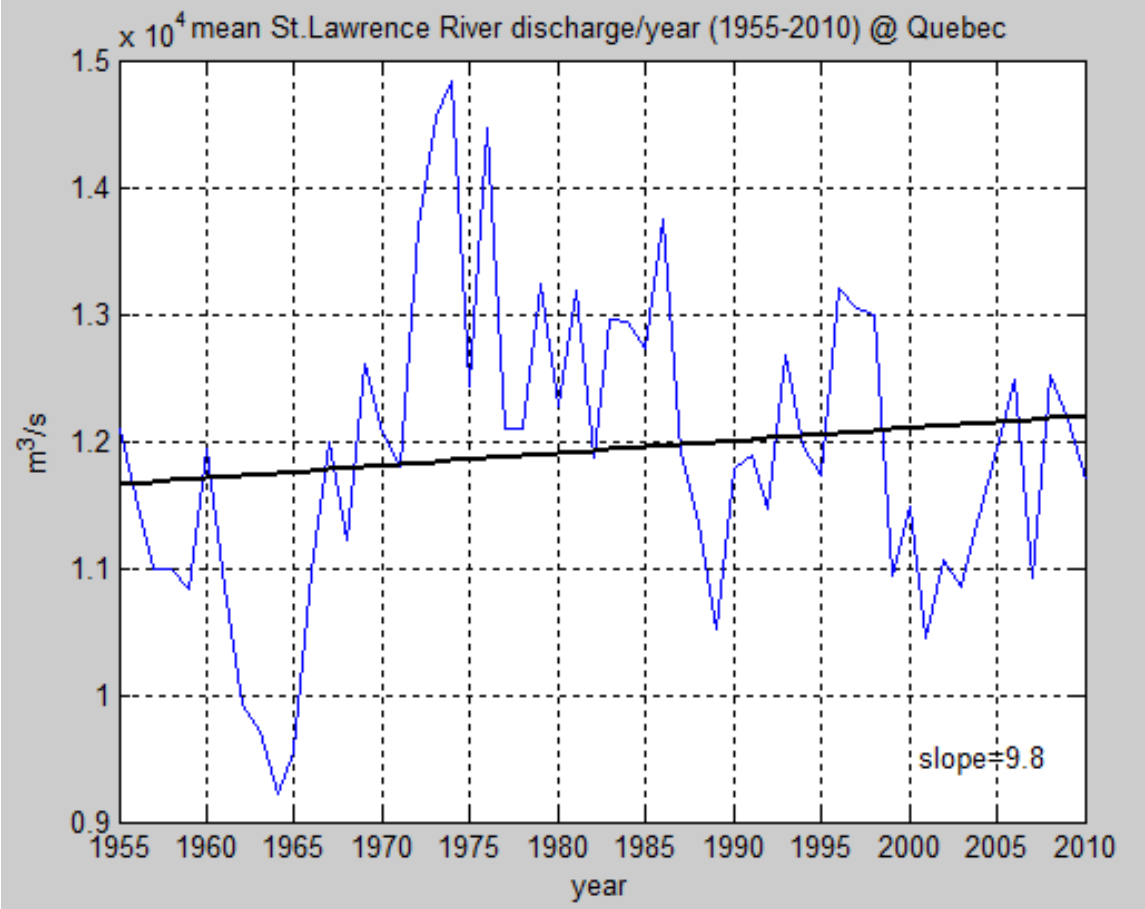

Figure 3.1: St. Lawrence runoff at Quebec City data obtained from slgo.ca (St. Lawrence Global Observatory)

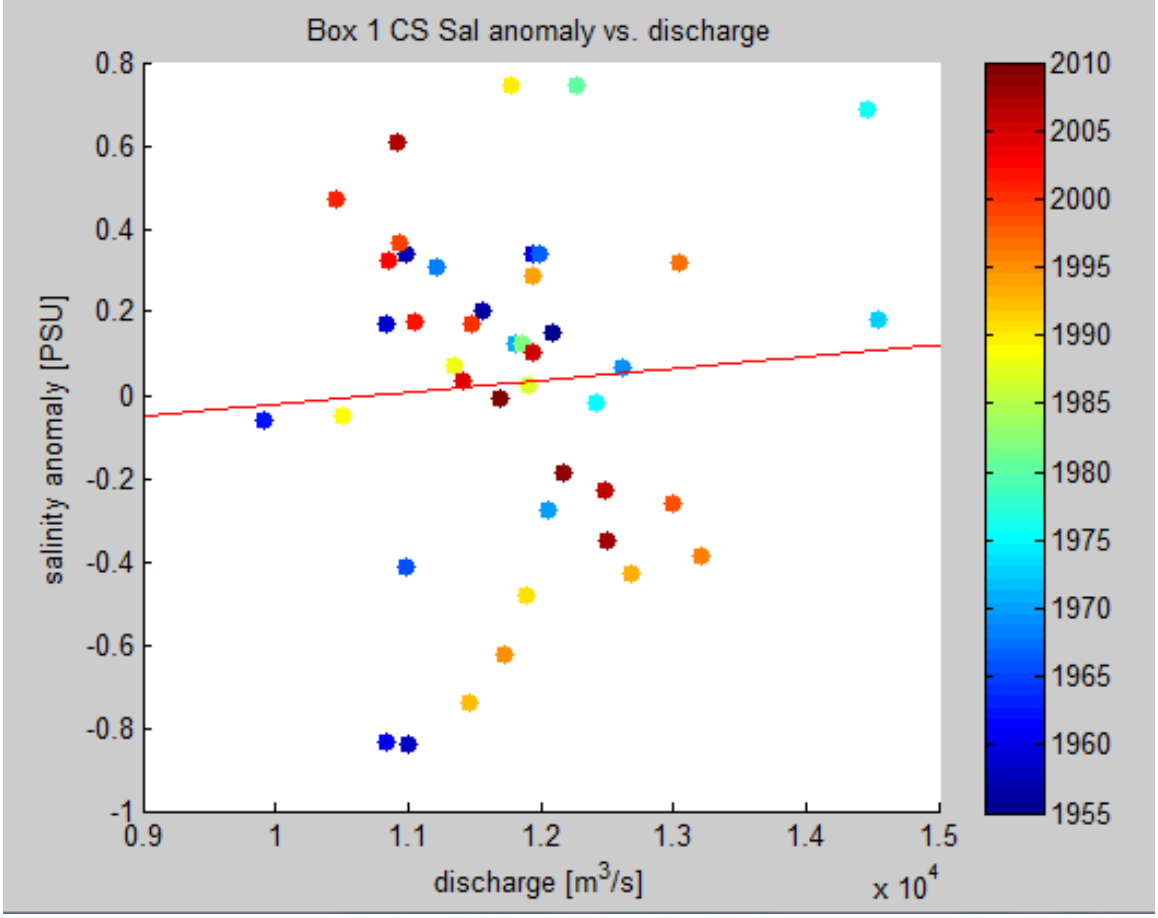

Figure 3.2 a: Box one salinity anomaly vs. discharge with linear regression. Box one encompasses the buoyancy driven current pathway

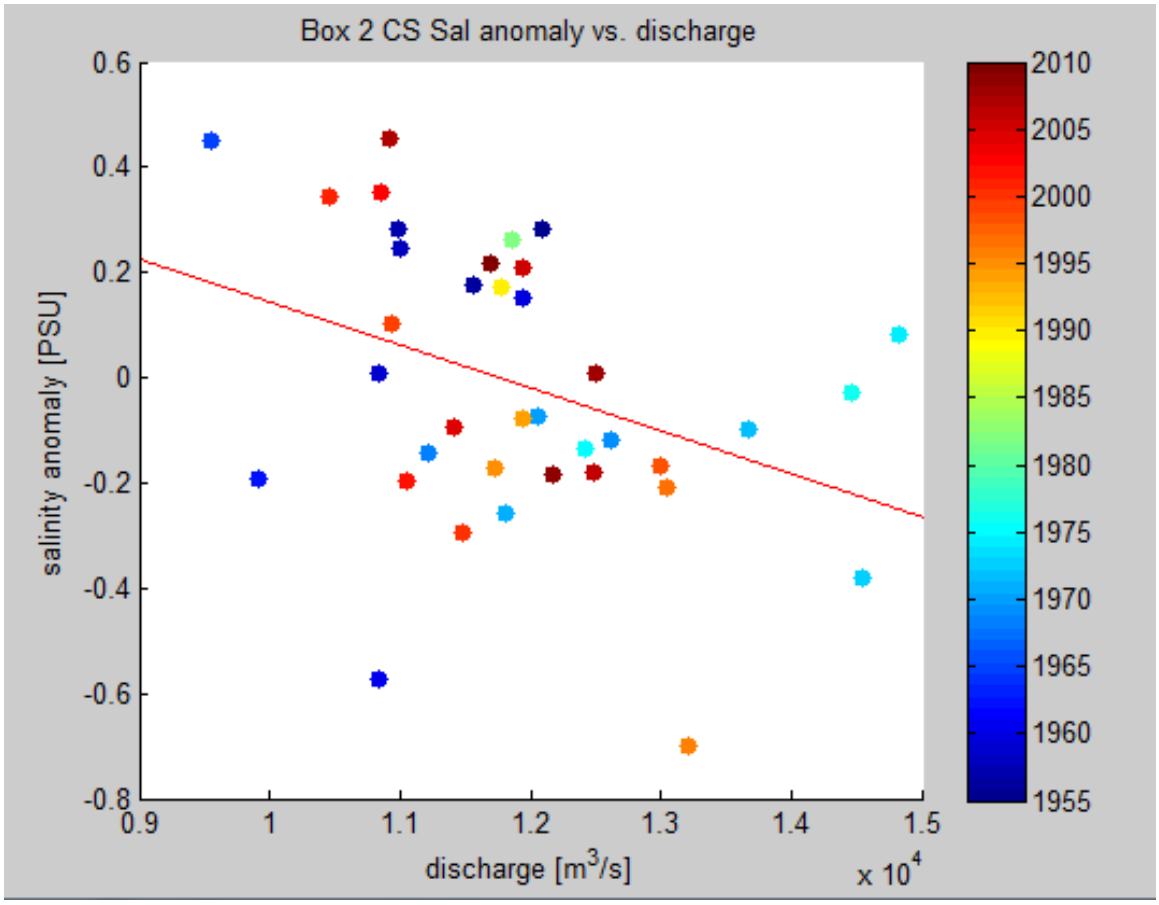

Figure 3.2 b: Box two salinity anomaly vs. discharge with linear regression. Box two encompasses local GSL waters as well as freshwater from the expanding plume during periodic occurring large freshwater releases

This study focused on the estuarine like circulation pattern in the GSL, where fresher water on the surface flowing seaward in linked with the advection of saltier water flowing landward at depth to maintain mass balance. The two main water masses that drive this circulation at the surface are the outflow from the St. Lawrence River system and the LC waters that are advected into the GSL through the SBI and the CS. We have not found a substantial change in the St. Lawrence River discharge rate, but as was shown by Fimmetta and Heimbach (2013), the LC has been undergoing changes.

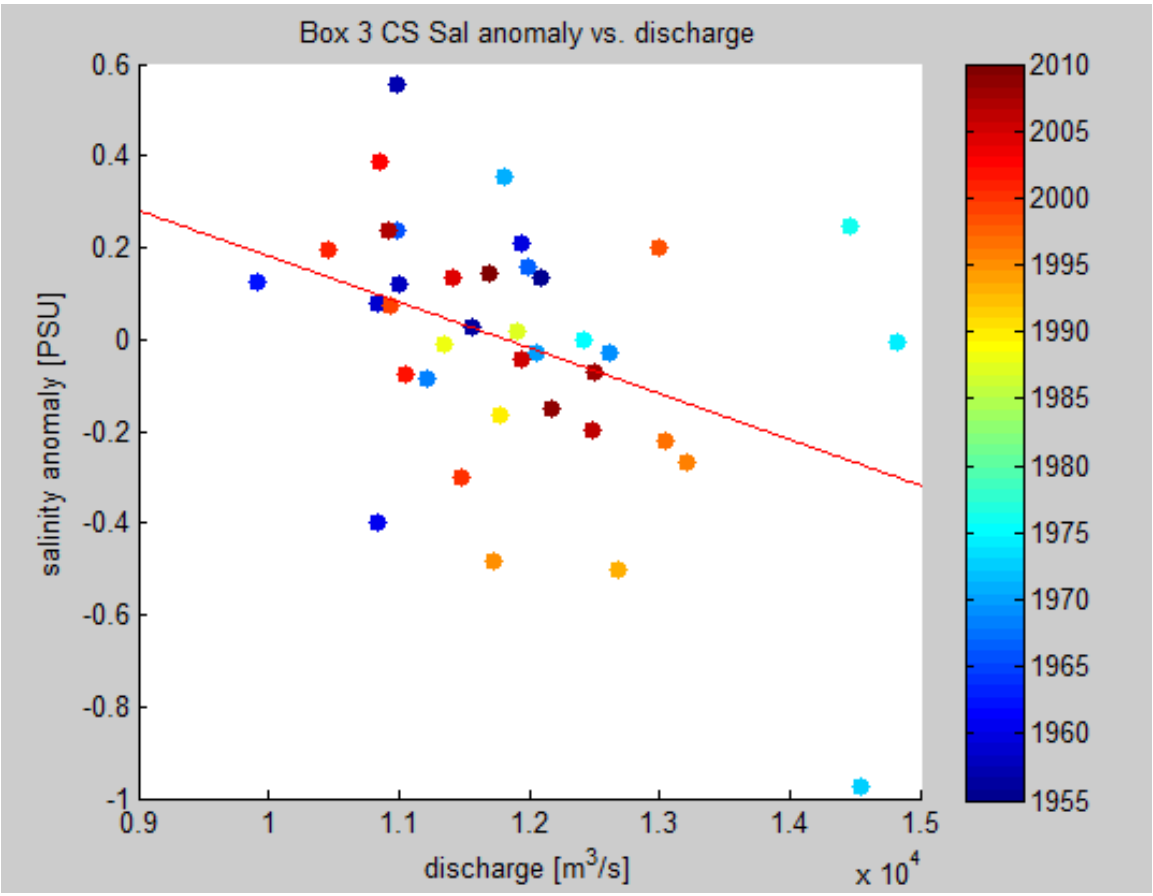

Figure 3.2 c: Box three salinity anomaly vs. discharge with linear regression. Box three encompasses GSL water pathway

They stated that “the mass loss from the Greenland ice sheet has quadrupled from 1992-2001 to 2002-2011”, leading to a freshening of the LC as a result of climate change. When we look at the boxes that are dominated by the LC influence, namely B3 at CS and B2 at AC as well as L1 at SBI, we can see a signature of this freshening trend. Especially B3 at CS shows a substantial warming and freshening trend. L1 at SBI also reflects this trend with a substantial warming and a non-substantial freshening. This freshening signal is a result of the LC receiving more freshwater from the increased melting rate of the Greenland ice sheet.

Our analysis did not show a drop in discharge but a slight increase for the whole time frame from 1955 to 2010. If we only look at the time frame from 1974 to 2010 it seems to show a slight decrease in discharge. The boxes that are occupied by the buoyancy outflow from the St. Lawrence River, namely B1 at CS and B1 at AC, show a clear trend towards salting and cooling. This trend can be explained by stronger mixing due to the increasing intensity of the atmospheric forcing (e.g. intensity and frequency of storm events) which is a result of the current climatic changes. These climate change-driven trends will become more pronounced over time; with an increase melting rate of the Greenland glaciers resulting in a freshening and probable warming of the LC and stronger and more frequent storms mixing freshwater runoff. Our analysis shows that global change trends can be enhanced in semi-enclosed basins due to advective processes.

If Mortsch and Quinns (1996) prediction of a decrease in runoff of the Great Lakes (which feed the St. Lawrence River) with increasing atmospheric CO_2 and a continuing increase of atmospheric forcing come true, we can expect the salting and

cooling trend of the buoyancy driven current to become even more pronounced. Mortsch and Quinn predict that an increase in temperature will lead to more evaporation which is then moved away from the great lakes drainage basin and results in less water raining over the Great Lakes watershed, in turn causing lower water levels and reduced outflow into the GSL. A significant drop in freshwater outflow from the St. Lawrence River will affect the GSL. We can already see stronger mixing resulting in a higher advection rate of compensating waters entering at depth. This trend would only be increased if the runoff diminishes. The IPCC 2014 report predicts a 5℃ temperature increase by the end of the 21st century for the GSL area (Wong et al. 2014), these predictions are in line with Mortsch and Quinns model who also predict an increase in temperatures leading to higher evaporation rates. Warming would also lead to an increase in frequency and intensification of atmospheric disturbances, which would further enhance the mixing of the surface water with saltier and cooler layers below. The perceived estuarine type circulation in the GSL would be intensified by such changes. By mixing and thereby salting the buoyancy driven current, the mass transport would be increased and in turn more water in the bottom layer would be advected in to compensate. The warming and salting trends of the bottom layer, that is consistent at all transects, reflects this increase of advection as a result to the changes occurring in the surface layer. The bottom waters have to compensate the increased flow rate at the surface, as a result of the freshwater flux and mass balance equations. The advection of more warm and saline water at depth leads to a stronger stratification between the deep layer and the CIL. This stratification slows down the mixing rate between the bottom layers. Mucci et al. (2011) found that the bottom waters of the GSL estuary are becoming hypoxic as well as becoming more acidic

showing that the stratification changes extends into the lower estuary. Increased acidification is a result of increased stratification, since it inhibits mixing and gas exchange with the surface and thus oxygenation of the deep layer. This trend could extend into the GSL where it would affect the ecosystem and thus local fisheries.

We also have not taken into account the role that local ice formation and melting plays. Local sea ice formation will add salinity through brine rejection and add freshwater to the surface layer when it melts. It would be interesting to include these variables in future studies since a change in local sea ice formation is most likely. With the predicted increase in average temperatures for the area of the GSL sea ice will form later in the season and thaw earlier.

The IPCC 2014 (Wong et al., 2014) report also predicts that sea lever will be rising on the northeastern American coast. Such a change will play a role in the future development of the GSL. One prevailing theory is that the difference in sea level at SBI is a driving force for waters entering the GSL (Galbraith P.S., 2006). If sea level increases it will have an effect on the SBI inflow rate, and the SBI is one of the major pass ways for water entering the GSL.

3.3 *CONCLUSION*

We used temperature and salinity data collected in the GSL from NOAAs National Oceanographic Data Center (NODC) for the warm season (May – October) during the 1950 – 2010 time period. Three transects were selected to encompass the major in and out flow water pathways. The grid size of the transects had a spatial dimensions of 10m depth, 10km cross channel and 50km along channel. The yearly

means were used to construct climatological transects for temperature and salintiy. Temperature and salinity data from each transect were sorted into bi-monthly bins. Means of each bi-monthly period were established for the entire time series. The bi-monthly means were utilized to calculate yearly non-biased anomalies for each layer and box. The GSL has a perceived estuarine type circulation, a fresh surface layer that flows seaward and a compensating flow at depth that flows landward. The surface layer has 2 major sources of buoyant water, one is the freshwater discharge from the Great Lakes through the St. Lawrence River and its estuary, feeding a buoyancy driven current on the west side of the basin; the second is the ambient water in the GSL, which have a signatures from the LC, with relatively fresh shelf water entering through the SBI and CS.

We found a freshening and warming trend in the non-locally forced ambient water of the GSL. This trend is a signal from the overall freshening of the LC, which in turn has been freshening as a result of the increased melting of the Greenland ice sheet. The Great Lake discharge rate itself has not changed drastically, which lead us to the hypothesis that the salting and cooling trends we found stem from an increased vertical mixing of said freshwater discharge, caused likely by intensifying atmospheric forcing. An increase in atmospheric forcing events intensity and frequency has been predicted and is seen as a sign of accelerating climate change; the increased mixing (and hence the salting) of the buoyancy driven current leads to an increased compensating flow at depth. Our results reflect the increased in-flow rate at depth as an increasing of temperature and salinity trends. This out/inflow coupling fits with a classical estuarine type circulation regime.

In conclusion our study found that current climatic changes have a strong influence on the GSL. Local forcing (buoyancy driven current) is affected through an increased mixing (caused by stronger and more frequent storms) as well as a non-local forcing (via the LCs freshening). We did not include local ice formation and melting or sea level rise in our analysis, although these factors are affected by climate change and in turn affect the GSL and should be included in future studied of the area. The occurring changes that we included in our analysis show a trend towards a stronger stratification of the GSL, with possible impact on the biology and the fisheries that are dependent on it. It will also change the characteristics of the outflowing waters onto the shelf and the effects will be propagated further downstream. We think that the GSL should be studied further, since its estuarine type circulation could be amplifying the climatic changes.

REFERENCES

Banks, R.E. (1966), The cold intermediate layer of the Gulf of St. Lawrence, Journal of Geophysical Research, Vol. 71, p. 1603 – 1610,

Bourgault, Daniel, and Vladimir G. Koutitonsky. "Real-time Monitoring of the Freshwater Discharge at the Head of the St. Lawrence Estuary." Atmosphere-Ocean 37, no. 2 (June 1999): 203–20. doi:10.1080/07055900.1999.9649626.

Bugden G.L. (1991), Changes in the temperature-salinity characteristics of the deeper waters of the Gulf of St. Lawrence over the past few decades, Canadian Journal of Fisheries and Aquatic Sciences, Vol. 113, p. 139 – 147,

Drinkwater, K F, and D Gilbert. "Hydrographic Variability in the Waters of the Gulf of St. Lawrence, the Scotian Shelf and the Eastern Gulf of Maine (NAFO Subarea 4) During 1991-2000." Journal of Northwest Atlantic Fishery Science 34 (September 24, 2004): 85–101. doi:10.2960/J.v34.m545.

El Sabh M.I. (1977), Oceanographic features, currents and transport in Cabot Strait, Canadian Journal of Fisheries and Aquatic Sciences, Vol. 34, p. 516 – 528,

Fiammetta, and Patrick Heimbach. "North Atlantic Warming and the Retreat of Greenland's Outlet Glaciers." Nature 504, no. 7478 (December 4, 2013): 36–43. doi:10.1038/nature12854.

Galbraith P.S., Larouche P., Chasse J., Petrie B. (2012), Sea Surface temperature in relation to air temperature in the Gulf of St. Lawrence: Interdecadal variability and long term trends, Deep – Sea Research II, Vol. 77-80, p.10-20

Galbraith, P.S. (2006), Winter water masses in the Gulf of St. Lawrence, Journal of Geophysical Research, Vol. 111, C06022,

Garret C. (1980), Dynamical Aspect of the Flow Through the Strait of Belle Isle, Journal of Physical Oceanography, Vol. 11, p. 376 - 392,

GeoMapApp: Ryan, W.B.F., S.M. Carbotte, J.O. Coplan, S. O'Hara, A. Melkonian, R. Arko, R.A. Weissel, V. Ferrini, A. Goodwillie, F. Nitsche, J. Bonczkowski, and R. Zemsky (2009), Global Multi-Resolution Topography synthesis, Geochem. Geophys. Geosyst., 10, Q03014, doi:10.1029/2008GC002332. http://www.geomapapp.org/

Gilbert D., Pettigrew B. (1997), Interannual variability (1948 – 1994) of the CIL core temperature in the Gulf of St. Lawrence, Canadian Journal of Fisheries and Aquatic Sciences, Vol. 54.S1, p. 57 – 67

Han, Guoqi. "Three-Dimensional Seasonal-Mean Circulation and Hydrography on the Eastern Scotian Shelf." Journal of Geophysical Research 108, no. C5 (2003). doi:10.1029/2002JC001463.

Han, Guoqi, John W. Loder, and Peter C. Smith. "Seasonal-Mean Hydrography and Circulation in the Gulf of St. Lawrence and on the Eastern Scotian and Southern Newfoundland Shelves." Journal of Physical Oceanography 29, no. 6 (1999): 1279–1301.

Han, Guoqi, Charles Hannah G., John W. Loder, and Peter C. Smith. "Seasonal Variation of the Three-Dimensional Mean Circulation over the Scotian Shelf." Journal of Geophysical Research 102, no. C1 (January 15, 1997): 1011–25.

Khatiwala S.P., Fairbanks R.G., Houghton R.W. (1999), Freshwater sources to the coastal ocean off northeastern North America: Evidence from H218O/H216O, Journal of Geophysical Research, Vol. 104, No. C8, p. 18.241 – 18.255

Ketchum, Bostwick H (1983), Estuaries and Enclosed Seas. Amsterdam: Elsevier Scientific Pub., 1983. Print.

Koutitonsky V.G., Bugden G.L. (1991), The Physical Oceanography of the Gulf of St. Lawrence: A review with Emphasis on the Synoptic Variability of Motion, Canadian Special Publication of Fisheries and Aquatic Sciences, Vol. 113, p.57 – 90

Linder C.A., Gawarkiewicz G. (1998), A climatology of the shelfbreak front in the Middle Atlantic Bight, Journal of Geophysical Research, Vol. 103, No.C9, p.18.405-18.425

Loder, John W., Petrie B., Gawarkiewicz. "The Coastal Ocean off Northeastern North America: A large-scale view" The Sea, Volume 11. Ed. Allan R. Robinson and Kenneth H. Brink ,1998. 105-133. Print

Mortsch, Linda D., and Frank H. Quinn. “Climate Change Scenarios for Great Lakes Basin Ecosystem Studies.” Limnology and Oceanography 41, no. 5 (1996): 903–11.

Mucci, Alfonso, Michel Starr, Denis Gilbert, and Bjorn Sundby. “Acidification of Lower St. Lawrence Estuary Bottom Waters.” Atmosphere-Ocean 49, no. 3 (September 2011): 206–18. doi:10.1080/07055900.2011.599265.

NODC National Oceanographic Data Center Home Page - http://www.nodc.noaa.gov/

Ohashi, Kyoko, and Jinyu Sheng. “Influence of St. Lawrence River Discharge on the Circulation and Hydrography in Canadian Atlantic Waters.” Continental Shelf Research 58 (April 2013): 32–49. doi:10.1016/j.csr.2013.03.005.

Petrie, Brian, and Kenneth Drinkwater. “Temperature and Salinity Variability on the Scotian Shelf and in the Gulf of Maine 1945–1990.” Journal of Geophysical Research: Oceans (1978–2012) 98, no. C11 (1993): 20079–89.

Petrie B., Toulany B. (1988) The Transport of Water, Heat and Salt Through the Strait of Belle Isle, Atmosphere – Oceans 26 (2), p.234 – 251

Romero-Lankao, P., J.B. Smith, D.J. Davidson, N.S. Diffenbaugh, P.L. Kinney, P. Kirshen, P. Kovacs, and L. Villers Ruiz, 2014: North America. In: Climate Change 2014: Impacts, Adaptation, and Vulnerability. Part B: Regional Aspects. Contribution of Working Group II to the Fifth Assessment Report of the Intergovernmental Panel on Climate Change [Barros, V.R., C.B. Field, D.J. Dokken, M.D. Mastrandrea, K.J. Mach, T.E. Bilir, M. Chatterjee, K.L. Ebi, Y.O. Estrada, R.C. Genova, B. Girma, E.S. Kissel, A.N. Levy, S. MacCracken, P.R. Mastrandrea, and L.L.White (eds.)]. Cambridge University Press, Cambridge, United Kingdom and New York, NY, USA, pp. 1439-1498.

Saucier F. J., Roy F., Gilbert D. (2003), Modeling the formation and circulation processes of water masses and sea ice in the Gulf of St. Lawrence Canada, Journal of geophysical Research, Vol 108, No. C8, p. 25-1 – 25-20

Saucier F.J., Chassé J. (2000) Tidal Circulation and Bouyancy effects in the St. Lawrence Estuary, Atmosphere – Ocean, Vol. 38 (4), p.505 – 556

Shaw J., Gareau P. Courtney R.C., (2002), Palaeogeography of Atlantic Canasa 13 – 0 kyr, Quaternary Science Reviews 21 (2002), p.1861-1878,

Skliris, Nikolaos, Robert Marsh, Simon A. Josey, Simon A. Good, Chunlei Liu, and Richard P. Allan. “Salinity Changes in the World Ocean since 1950 in Relation to

Changing Surface Freshwater Fluxes." Climate Dynamics 43, no. 3–4 (August 2014): 709–36. doi:10.1007/s00382-014-2131-7.

Smith, G. C., F. J. Saucier, and D. Straub. "Formation and Circulation of the Cold Intermediate Layer in the Gulf of Saint Lawrence." Journal of Geophysical Research 111, no. C6 (2006). doi:10.1029/2005JC003017.

St. Lawrence Global Observatory: www.slgo.ca

Tang C.L. (1983) Cross – Frontal Mixing and frontal Upwelling in a Controlled Quasi – Permanent Density Front in the Gulf of St. Lawrence, Journal of Physical Oceanography, Vol. 13, p.1468 – 1481

Tang C.L. (1980), Mixing and Circulation in the Northwestern Gulf of St. Lawrence: A Study of a Buoyancy – Driven Current System, Journal of Geophysical Research, Vol. 85, No. C5, p. 2787 – 2796, 1980

Wang J., Ingram R.G., Mysak L.A. (1991), Variability of Internal Tides in the Laurentian Channel, Journal of Geophysical Research, Vol. 96, No. C9, p. 16.859 – 16.875

Wong, P.P., I.J. Losada, J.-P. Gattuso, J. Hinkel, A. Khattabi, K.L. McInnes, Y. Saito, and A. Sallenger, 2014: Coastal systems and low-lying areas. In: Climate Change 2014: Impacts,Adaptation, and Vulnerability. Part A: Global and Sectoral Aspects. Contribution of Working Group II to the Fifth Assessment Report of the Intergovernmental Panel on Climate Change [Field, C.B., V.R. Barros, D.J. Dokken, K.J. Mach, M.D. Mastrandrea, T.E. Bilir, M. Chatterjee, K.L. Ebi, Y.O. Estrada, R.C. Genova, B. Girma, E.S. Kissel, A.N. Levy, S. MacCracken, P.R. Mastrandrea, and L.L.White (eds.)]. Cambridge University Press, Cambridge, United Kingdom and New York, NY, USA, pp. 361-409.

Xu X., Hurlburt H.E., Schmitz Jr., Zantopp R. Fischer J., Hogan P.J. (2013), On the currents and transports connected with the atlantic meridional verturning circulation in the subpolar North Atlantic, Journal of Geophysical Research: Oceans, Vol. 118, p.502-516